Blending of Polyhydroxybutyrate-co-valerate with Polylactic Acid for Packaging Applications – Reflections on Miscibility and Effects on the Mechanical and Barrier Properties

V. Jost[a,*] and R. Kopitzky[b]

[a]Fraunhofer Institute for Process Engineering and Packaging IVV, Giggenhauser Strasse 35, 85354 Freising, Germany

[b]Fraunhofer Institute for Environmental, Safety, and Energy Technology UMSICHT, Osterfelder Strasse 3, 46047 Oberhausen, Germany

doi: 10.15255/CABEQ.2014.2257

Original scientific paper
Received: July 4, 2014
Accepted: June 10, 2015

Biopolymers for packaging applications offer many advantages and are therefore of increasing interest. In order to develop a sustainable alternative for petrochemical-based polymers the biobased and biodegradable polymers, the focus of this work are polyhydroxybutyrate-co-valerate (PHBV) and polylactic acid (PLA) (and copolymers). Blending of these two biopolymers was reviewed under thermodynamic aspects and backed with own results. Additionally, different ways of improving the miscibility were performed by compatibilisers, peroxides, transesterification catalysts, and by blending PHBV with modified molecular weight. These blends were extruded as cast films, and characterised by means of mechanical and barrier properties. This study analyses the miscibility of PLA and PHB-copolyester (with approximately equal molar masses) and reports on the unusually high barrier properties in PLA and PHBV blends. However, the quality of blending, especially regarding barrier properties to interphase boundaries, depends on the compatibility of the components and the morphology of the blend. Our results suggest that a PHBV content of 20–35 % in PLA is the most suitable blend system in terms of compatibility and high barrier properties.

Key words:

polyhydroxybutyrate-co-valerate, polylactic acid, blends, miscibility, mechanical properties, barrier properties

PLA and PHBV for packaging applications

Sustainable packaging is a growing market due to consumer awareness of 'green' packaging, facilitated availability of biopolymers and improved processability. Rising concerns regarding environmental and economic aspects of the use of petrochemical-based materials further increase the interest in their replacement by biopolymers. In order to develop a blend material suitable for scale-up to industrial dimensions, two entirely biobased, biodegradable, thermoplastic and commercial polymers with currently the best availability were chosen: polylactic acid (PLA) and polyhydroxybutyrate-co--valerate (PHBV). These base materials show opposing properties in their processing as well as mechanical and barrier properties (regarding water vapour, oxygen and aroma).[1] With the target of combing the mechanical strength of PLA with the high barrier properties of PHBV, blends of these polyesters should be developed. Thereby, the drawbacks of the individual polymers should be compensated.

Of special interest is the influence of blending on the barrier properties. For an overview, not only the oxygen and water vapour permeability of the developed blends was analysed, but also the permselectivity of the gases nitrogen, oxygen to carbon dioxide. The factor between these gases often determines the application possibilities, e.g. for food packaging.

PLA is known for its biocompatibility, biodegradability, high Young's modulus and transparency.[1] Depending on the isomeric content, the chemical as well as mechanical properties are changing. Additionally, the molecular weight influences the properties of this polar polymer.[2]

The second biopolymer applied in this study belongs to the group of polyhydroxyalkanoates (PHAs). They are water-insoluble storage polymers in microorganisms, presently produced by the fermentation of renewable carbon resources.[3–5] These linear polyesters exhibit thermoplastic properties.

* Corresponding author: Verena.Jost@ivv.fraunhofer.de; Phone +49 8161 491 227; Fax +49 8161 491 555; Rodion.Kopitzky@umsicht.fraunhofer.de

The basic structure is a C_3 chain with a carboxyl group forming the polyester backbone. The basic structure has at C-3 a side chain, which determines the type of PHA. The most commonly used PHAs are polyhydroxy-butyrate (PHB, C_4) with a methyl group as side chain, or poly-3-hydroxybutyrate-co-3--hydroxyvalerate (PHBV, C_4 resp. C_5) which is a copolymer of PHB and PHV with a methyl or ethyl side chain, respectively. Due to the longer side chain of PHV in comparison to PHB the melting and glass transmission temperatures are decreased, which leads to a lower crystallinity and better processing behaviour of the extremely thermosensitive PHB-(co)-polymers in an extrusion process.[1,6]

Mechanical and barrier properties of both PHB and PHBV are shown in literature.[1,7] The water vapour transmission rate (WVTR) of PHBV-coated paper was revealed to be around four to six times lower than the equivalent of LDPE.[8] This was partly explained as a result of the high polarity of PHBV. For PLA, it is known that the barrier properties are lower than those of PHBV.[1,9,10] Tsuji and Tsuruno[11] stated WVTR of PLA films with a thickness of 25 μm of 98 – 224 g m^{-2} d^{-1} depending on their ratio of stereocomplexes.

In order to develop biopolymer blends with good processability and high barrier properties, different approaches are possible. These approaches to further improve the less than optimal intrinsic properties of PHAs or PLA can be named by chemical (PLA) or biochemical (PHBV) molecular design of the polymer backbone, which are time consuming and expensive, or the usage of sophisticated composite structures. The latter is a combination of two PHBV layers with an 'interlayer of electrospun zein nanofibres'.[12] However, from an industrial applicability point of view, it is advisable to ease the processing and further conversion by applying a commercialised and well-processable material. By combining the two biopolymers in a blend system, the goal is to produce a processable biopolymer material with high barrier properties. Thereby, the advantages of PLA (good availability, good processability) and PHBV (comparably high barrier properties) may improve the blends' properties, so that material usage is decreased and application possibilities are broadened. Recently, a few authors have taken up this approach and reported about barrier properties of PLA and PHBV blends.[13,14]

With the aim of combining the advantages of these two base materials, different blending strategies to improve their miscibility and properties are the focus of this study. Thus, we analysed the effect of different compatibilisers, peroxides, and transesterification catalysts, as well as the influence of modified PHBV.

However, it must be brought to mind that the blend components should be compatible with each other. In particular, the permeability of the gases may be altered by insufficient miscibility due to a lack in interfacial adhesion. For PLA and PHBV several studies on miscibility can be found in literature.[13,15–45] Concerning thermodynamic aspects, the reported solubility parameter differences are in the range of 0.34 to 0.8 $J^{0.5}$ $cm^{-1.5}$ and different conclusions on miscibility and immiscibility reveal a need for clarification.

Therefore, the aim of this work is to summarise published data and report our experimental data on miscibility (part I), and mechanical and barrier properties of PHBV and PLA blends (part II), prepared by solution casting and cast film extrusion.

Materials and methods

Materials

L-Polylactic acid (PLA) was obtained from NatureWorks LLC (type 2002D), Minnetonka, USA by its distributor Resinex Germany GmbH, Zwingenberg, Germany. According to own measurements, this grade has a molecular weight M_w of 205 kDa and M_n of 110 kDa. No melting temperature was given in the data sheet.

PHBV (ENMAT™ Y1000P) from Ningbo Tianan Biologic Material Co., LTD in Ningbo, China was obtained from Peter Holland BV, Venlo, Netherlands. The molecular weight was 240 kDa for M_w and 92 kDa for M_n according to own measurements. The T_m was between 170 – 176 °C, the content of valeric acid was approx. 3 % according the data sheet.

Both polymers were dried at 70 °C for 4 hours before blending. All materials were pre-dried before extrusion at 60 °C for at least 12 hours.

Depolymerisation of the polymers was done in analogy to a procedure described by Wu, Chen [46] by acid catalysed methanolysis in chloroform at boiling temperature. Due to (basic) additives in the commercial plastic types, the depolymerisation time was prolonged. An amount of 30 g of polymers were dissolved in 400 mL of chloroform, and in steps of about 60 minutes 50-mL samples were taken and precipitated in a five-fold excess of ethanol. The precipitated polymers were filtered in vacuum, washed with ethanol, and dried at a rotary pump for several hours at 10^{-2} mbar at elevated temperatures (~ 60 °C in a water bath) unless no characteristic IR bands of chloroform and ethanol were seen.

Low molecular weight PLA was also synthesised by the reaction of commercial PLA (M_n~ 110 kDa) with lactic acid (80 %) in a weight ratio of

10:1 under Argon at 190 °C. One sample was taken after melting and homogenisation of the mixture (~ 80 minutes), and 5 hours later (* s. b.). The first sample had a higher molecular weight and dispersity (see below, 15 kDa sample). In a second depolymerisation step, commercial PLA was hydrolysed with oligomeric lactic acid of M_n = 1.2 kDa in a weight ratio of 6.6:1 at 190 °C under Argon. Samples were taken at 2.5 and 5h after melting and homogenisation of the mixture (~ 80 min) (** s. b.).

Samples with a number average molecular weight (M_n) in kDa of 37.5 (1.5), 35 (1.6), 32 (1.8), 27 (1.4)**, 19 (1.6)**, 15 (2.2)*, 7.5 (1.8)* for PLA and 39.5 (1.8), 33.5 (1.8), 28 (1.7), 23.5 (1.7), 15 (1.6) and 10 (1.6) were used for the miscibility study. Dispersion of molecular weight is mentioned in brackets.

Methods

Solution casting

Solution casting was done by dissolving 0.1 g polymer powder mixture in 2 mL boiling chloroform, and casting the hot solution on a warmed petri dish (60 °C) for fast evaporation of solvent, to inhibit gradiently the deposition of polymer fractions. The film was released and dried with a rotary pump at 10^{-2} mbar at elevated temperature for several hours unless no chloroform was detectable in the IR-spectrum.

Blending

Blending of PHBV and PLA for preliminary tests was done in an internal mixer (Brabender Plasticorder with mixer W350E). In PLA-rich blends, the mixer was filled first with PLA (in two steps) and after plastification of PLA, PHBV was added. The temperature of the mixing chamber for filling was set to 180 °C with a rotation speed of the blades of 40 rpm. During the plastification of PHBV, the temperature of the mixing chamber was set to 160 °C and the rotational speed of the blades were adjusted manually (remote control off) so that the melt temperature did not exceed 180 – 190 °C. PHBV-rich blends were first mixed with PLA as dry blends, and the mixer was filled in two steps. In the second step, the temperature of the mixing chamber was set from 180 °C to 160 °C and the temperature of the melt was adjusted as mentioned above. After plastification of all components, the additives were added.

For the reactive mixing, the stamp was replaced with a plate having gas inlet valves (hand-made) and the chamber was flushed with dry nitrogen before starting. During mixing, few mbar excess pressure of nitrogen was fixed. Insertion of peroxides was performed by the counterflow principle to avoid oxygen contamination.

Transesterification

Transesterification of PLA and PHBV was accomplished in an internal mixer (see above). A 50:50 mixture of about 320 g was reacted with 1 or 3 g of transesterification catalyst for 95 or 180 minutes.

Compounding

Compounding was done using an intermeshing co-rotating twin-screw extruder EMP 26–40 from TSA Industriale, Italy, with the screw diameter D being 26 mm and the screw length L 40 D. PLA, PHBV, and the additives were dry-blended and fed by a gravimetrical dosing feeder.

For compounding of compatibilisers, the heating zones were set to 160, 165, 170, 170, 170, 170, 170 and 170 °C, respectively, with a rotation speed of 200 rpm and about 10 kg h^{-1} output. Pressure on nozzle was about 14–19 bar and torque was 15–50 N m (15–23 PEG-PE; 40–50 PMMA).

For reactive extrusion with dicumyl peroxide the heating zones were set at 160, 170, 180, 190, 195, 195, 195 and 180 °C, respectively, with a rotation speed of 180 rpm and about 8–10 kg h^{-1} output. Pressure on the nozzle was about 11–19 bar and torque at 20–30 N m (rotational speed and temperatures up to 195 °C were selected due to half-life-time of peroxide, assuming a dwell time of about 8 seconds in each zone, and a mass temperature about 10 °C higher than wall temperature).

For compounding PLA and PHBV with a transesterificate of PLA and PHBV (see above), the temperature of the heating zones were set at 160, 170, 170, 180, 180, 180, 170 and 165 °C, respectively, with a rotation speed of 200 rpm and about 10 kg h^{-1} output. Pressure on nozzle was about 14–17 bar and torque was 20–30 N m.

Melt strands were extruded through a dual strand die (d_0 = 3 mm) into a water bath. The strands were pelletized and dried for 6 h at 70 °C with standard equipment.

Extrusion of cast films

The cast films were produced by a flat film extrusion plant (E 30 M) with a nozzle width of 300 mm and a barrel length of 30D of Dr. Collin GmbH, Ebersberg, Germany.

Conditioning

Before analysing, all samples were conditioned at a constant temperature, and humidity set at 23 °C with 50 % rh (relative humidity) for at least 48 h to adjust the moisture content.

Thickness measurements

The thickness of the extruded film samples was measured after conditioning by a Precision Thickness Gauge FT3 (Rhopoint Instruments, Bexhill on Sea, UK) providing a 0.4 μm repetition accuracy. Ten thickness measurements were taken on each sample at different positions. In the results, only the mean values are reported.

Differential Scanning Calorimetry (DSC)

Differential Scanning Calorimetry (DSC) was performed on a Netzsch DSC 204 F1 Phoenix DSC instrument (Netzsch Gerätebau, Selb, Germany). Each sample was melted at 190 °C for one minute and then rapidly quenched in liquid nitrogen for freezing the molten morphology. For evaporation of the condensate film on the crucible, which would disturb PHBV glass transitions, the samples were then annealed at room temperature for a few seconds, and cooled to –40 °C with 20 K min^{-1}. Heating was done with a heating rate of 10 K min^{-1} to 190 °C. The cooling step after the first heating was done at a rate of 20 K min^{-1} to –40 °C, which was followed by the second heating step at a rate of 10 K min^{-1}. A constant flow of nitrogen gas (20 mL min^{-1}) was used during the measurements. Analysis was done with the 'Netzsch Proteus – Thermal Analysis' software, version 6.

Size exclusion chromatography

Size exclusion chromatography was performed at an Agilent System at 25 °C with 1,1,1,3,3,3-hexafluoro-2-isopropanol (HFIP) containing 0.05 m potassiumtriflouroacetat (KTFAc) as solvent. The flow rate was fixed to 1 mL min^{-1} (isocratic pump G1310A, Agilent Series 1100). Detection was performed with a refractive index detector G1362 (Agilent Series 1100). PSS-PFG columns were used (PSS, Mainz, Germany: 7 μm, 1000 Å (8 × 300 mm), 7 μm, 300 Å (8 × 300 mm), 7 μm, 100 Å (8 × 300 mm)).

An amount of 9 mg of each sample was dissolved in 3 mL of HFIP, filtered with a 0.45 μm membrane and transferred to a vial. In the case of PHBV it helps to solve 15 mg of PHBV with 4 mL HFIP in a 5 mL graduated flask at boiling temperature and filling the flask after cooling to 5 mL.

An amount of 100 μL were injected (G1313A Agilent Series 1100). A narrow molecular weight distribution PMMA standard (PSS Mainz, Germany) was used as calibration. The curves were examined with the WinGPC®UniChrom (Version 8.1) Software (PSS, Mainz, Germany).

Mechanical properties

The Young's modulus (YM), tensile strength (σ), and elongation at break (ε) were measured according to DIN EN ISO 527–1 using a device Z005 Allround Line of Zwick GmbH & Co. KG, Ulm, Germany, with a load cell of 5 kN both in machine (MD), and in transversal direction (TD). Stripes of a width of 15 mm were cut of each sample, which were then inserted with an effective length of 100 mm between the clamps at the beginning of the measurement. In order to measure the tensile properties as a function of the film thickness, the thicknesses of each specimen was measured by a five-fold determination. The arithmetic mean and standard deviation of this determination were calculated. The samples were tested under monoaxial tensile stress at a velocity of 50 mm min^{-1}.

Oxygen permeability

The oxygen permeability (OP) was measured by a carrier gas (N_2) method (according to DIN 53 380 Part 3) in Oxtran Twin devices from Mocon Inc.. The amount of oxygen that permeates through a packaging material under constant conditions (23 °C, 50 % rh) is detected by an electrochemical sensor. A two-fold determination was performed in all cases and from these measurements, the standard deviation was calculated.

The OP values, Q, are given in cm^3 (STP) m^{-2} d^{-1} bar^{-1} and were converted to a normalised constant thickness, d, of 100 μm (Q_{100}) using the following equation in order to allow direct comparison of different samples independent of the film thickness. Therefore, the unit of the discussed Q_{100} is cm^3 (STP) 100 μm m^{-2} d^{-1} bar^{-1}.

$$Q_{100} = Q \cdot \frac{d}{100} \tag{1}$$

Additionally, the permeability against different gases was analysed with oxygen (OP), nitrogen (N_2-P) and carbon dioxide (CO_2-P) by a manometric method (according to DIN 53 380 Part 2) in GDP/E devices from Brugger Feinmechanik GmbH, München, Germany. The permeability was analysed by the amount of gas that permeates through the material under constant conditions (23 °C, 0 % rh) by the velocity of the increase of the partial pressure after pressure variation in the permeation cell. A two-fold determination was performed in all cases and from these measurements, the standard deviation was calculated. The Q_{100} was calculated according to Equation 1.

Water vapour permeability

The water vapour transmission rate (WVTR) was determined by a gravimetric measurement (according to DIN 53 122–1). Therefore, the amount of water vapour that permeates through a sample under constant conditions (23 °C, 85 → 0 % rh) is measured. A four-fold determination was performed on each sample. For statistical analysis, the standard deviation was calculated. The measuring area of the samples was 50.26 cm^2. The humidity inside the cups (0 % rh) was fixed by silica gel, and the external conditions (85 % rh) by a climate chamber of Binder GmbH.

The WVTR values, Q, are given in g m^{-2} d^{-1} and were converted to the normalised thickness d of 100 µm (g 100 µm m^{-2} d^{-1}) by using Equation 1. To be in accordance with S.I. units, and to gain the water vapour permeability (WVP), the WVTR can be divided by the humidity gradient at the applied conditions (23.919 mbar). For a better comparison with literature data, in this study the WVTR was used.

Miscibility under the aspect of thermodynamics and a small executive summary on former publications

Miscibility

Many publications deal with the miscibility of PLA and PHB and the copolyesters of PHB like PHBV[13,15–45] but only two publications consider the thermodynamic aspects.[30,35] Using the theory of Flory[47,48] and Huggins[48,49] for miscibility, the following equation is applied:

$$\frac{\Delta G}{R \cdot T \cdot V} = \left(\frac{\Phi_1}{V_{1m}} \cdot \ln \Phi_1 + \frac{\Phi_2}{V_{2m}} \cdot \ln \Phi_2 + \frac{\Phi_1 \cdot \Phi_2}{R \cdot T} (\delta_1 - \delta_2)^2 \right); \quad (2)$$

$$(\delta_1 - \delta_2)^2 = \frac{R \cdot T}{V_m} \cdot \chi_{12}$$

Where ΔG is the free enthalpy of mixing, R the gas constant, V the volume of the system, Φ_1 and Φ_2 are, respectively, the volume fractions, V_{1m} and V_{2m} are, respectively, the molar volumes, δ_1 and δ_2 are, respectively the solubility parameters, and χ_{12} the Flory-Huggins Interaction parameter. Miscibility depends on molecular weights, temperature and volume fraction of the components, and can be predicted on the basis of the knowledge of the solubility parameters or the – mostly unknown – interaction parameter χ_{12}, which includes specific interactions between the polymers. From a theoretical point of view, often the solubility parameters are used to calculate miscibility for a first insight. Using incremental parameters resting upon datasets for molecular groups developed by several authors[50–53] as listed in the book of Robeson[48], a difference in the solubility parameters of around 0.3–0.4 up to 0.8–0.9 $J^{0.5}$ $cm^{-1.5}$ can be calculated assuming non-polar interactions (see Table 1). For a blend of polyesters, dipol-dipol interactions can be assumed and a solubility parameter difference of up to 0.5 $J^{0.5}$ $cm^{-1.5}$ should allow miscibility.[52] Therefore, using only the data of van Krevelen,[50] miscibility should be given and, using the data of Hoy[53] immiscibility is stated. As a consequence, the mean of the data of van Krevelen,[50] Small,[51] Coleman[52] and Hoy[53] as given in Table 1, is used for a first estimation of miscibility. The calculated values of about 0.65 and 0.59 $J^{0.5}$ $cm^{-1.5}$ for the rubbery state and the glassy state are slightly above the allowed difference of solubility as stated by Coleman.[52] Therefore, a critical dependence of molecular weights and temperature should exist.

Table 1 – *Solubility parameters of PLA and different PHA grades*[48]

Calculated Solubility Parameter [$J^{0.5}$ $cm^{-1.5}$]						
Rubbery state	Small	Hoy	Van Krevelen	Coleman	Mean	Δ mean
PLA	19.72	20.05	18.69	18.82	19.32	
PHB	19.01	19.21	18.32	18.24	18.69	0.63
PHBV (5%V)	18.98	19.18	18.30	18.22	18.67	0.65
PHBV (15%V)	18.93	19.12	18.28	18.17	18.62	0.70
Glassy state						
PLA	20.04	20.37	18.99	18.82	19.55	
PHB	19.40	19.61	18.70	18.24	18.99	0.56
PHBV (5%V)	19.38	19.58	18.69	18.22	18.97	0.59
PHBV (15%V)	19.33	19.53	18.67	18.17	18.92	0.63

In Figures 1a and b, the free Gibbs energy according to Flory-Huggins – using a solubility parameter difference of 0.65 $J^{0.5}$ $cm^{-1.5}$ – is shown for several combinations of molecular weights of PLA and PHBV, as an example. It is clearly shown that miscibility over the whole range will only be possible with molecular weights of the polyesters below ~ 25 kDa, and partly miscibility should be allowed up to molecular weights of polyesters of 50 kDa. Partial miscibility of some amounts of polyester 1 in polyester 2 depends on the relative molecular weight of the polyesters, but the low molecular weight polyester dominates the miscibility.

Taking miscibility over the whole range of composition into account, the spinodal condition is often used:[48]

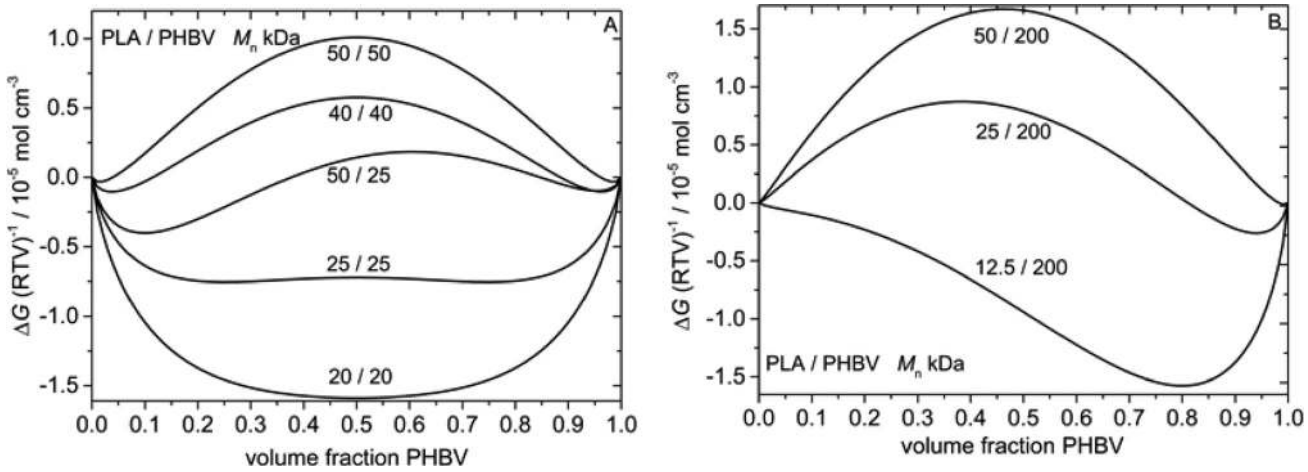

Fig. 1 – *Free enthalpy of mixing at 190 °C of PLA and PHBV according to Flory-Huggins theory and a difference in solubility parameter of 0.65 J$^{0.5}$ cm$^{-1.5}$ and density of both polymers of ρ = 1.25 g cm^{-3} in dependence of molecular weight (kDa, figures at the curves); a: general influence, b: influence of low molecular weight components*

$$\frac{\partial^2 G}{\partial \Phi_i^{\,2}} = R\cdot T\cdot V\left(\left(\frac{1}{V_{1m}\cdot\Phi_1}+\frac{1}{V_{2m}\cdot\Phi_2}\right)-2\cdot\frac{(\delta_1-\delta_2)^2}{R\cdot T}\right)=0;$$

$$\rightarrow T=\frac{2\cdot(\delta_1-\delta_2)^2}{R}\left(\frac{V_{1m}\cdot\Phi_1\cdot V_{2m}\cdot\Phi_2}{V_{1m}\cdot\Phi_1+V_{2m}\cdot\Phi_2}\right) \qquad (3)$$

Figure 2 shows the temperature needed for miscibility in dependence of molecular weights and volume fractions, and shows the sensitive influence of low molecular weight fractions.

The published results of several authors are summarized in Table 2. It reveals that many of the blends marked as immiscible consist of two high molecular weight components, and the blends marked as miscible consist of at least one part of low or very low molecular mass. Therefore, conclusions about miscibility or immiscibility in the PLA-PHBV-system are not very reliable concerning blends with applied relevance in construction materials for extrusion or injection moulding.

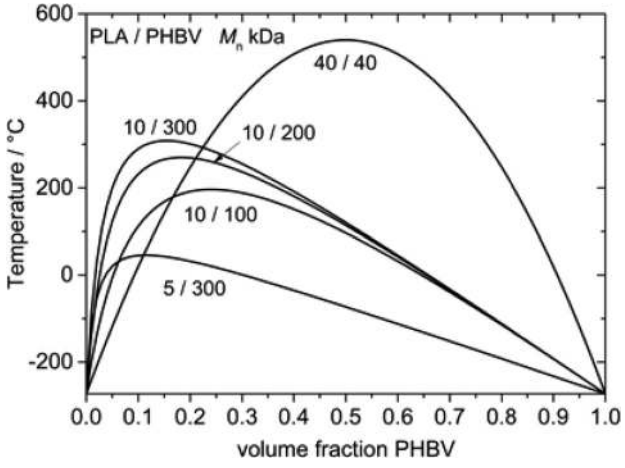

Fig. 2 – *Spinodal curves for binary blends of PLA and PHBV using a solubility parameter difference of Δδ = 0.65 J$^{0.5}$ cm$^{-1.5}$ and density of both polymers of ρ = 1.25 g cm^{-3}; molecular weights (kDa) are presented at the curves*

The critical point where the spinodal and binodal curve of the phase diagram intersects and miscibility over the whole range is achieved, is defined by Robeson[48] as follows:

$$\frac{\partial^3 G}{\partial \Phi^3}=0\rightarrow\Phi_{2,cr}=\frac{V_{1m}^{0.5}}{V_{1m}^{0.5}+V_{2m}^{0.5}} \qquad (4)$$

From this condition, the critical value for the difference of solubility parameters can be calculated by substituting the volume fractions in the spinodal condition.[48]

$$(\delta_1-\delta_2)_{cr}^2=\frac{R\cdot T}{2}\left(\frac{1}{V_{1m}^{0.5}}+\frac{1}{V_{2m}^{0.5}}\right)^2 \qquad (5)$$

This critical difference of solubility parameters of the polymers is included in Table 2. The number average molecular weights (M_n) were used for this calculation. For blends marked as immiscible, these parameters show the maximum allowed difference in the solubility parameter of PHBV and PLA in relation to their molar volumes (related to their molecular weight by density). Therefore, the true solubility parameter difference of PHBV and PLA should be higher than the calculated value in immiscible-marked blends. In miscible blends, the true solubility parameter difference may be less than the calculated critical difference in the solubility parameters. The values in Table 2 reveal that the solubility parameter difference should be between ~ 0.3 and ~ 0.8 J$^{0.5}$ cm$^{-1.5}$. Only a few literature data available indicate a solubility parameter difference of about 0.4 to 0.7 J$^{0.5}$ cm$^{-1.5}$. Comparing our results with literature data, we concluded that the calculated difference of solubility parameter by Koyama[30] seems to be too low, but this may be due to an

typing error (0.54 instead of 0.34 and using M_n instead of M_w because Figures 3 in their paper cannot be reproduced with this number). However, the data of Blümm and Owen[17] seems to be too high.

Also included in Table 2 is the *k*-parameter of the Gordon-Taylor equation (G-T-equation, equation 6)[55–57] for calculating the glass-transition temperature (T_g) of the blend. Data for the whole composition or data for the partial miscible compositions from literature is used (at least one blend composition is needed):

$$T_g = \frac{w_1 \cdot T_{g1} + k \cdot w_2 \cdot T_{g2}}{w_1 + k \cdot w_2}; \quad (if\ k = \frac{T_{g1}}{T_{g2}}\ then\ T_g = \frac{w_1}{T_{g1}} + \frac{w_2}{T_{g2}}\ Fox\ \ equation) \tag{6}$$

The G-T-equation is based on volume and free volume additivity[57] and considers the temperature-dependent volume fractions of the blend, leading to corrected temperature-independent weight fractions.[57] The constant *k* can be interpreted in well-defined molecular terms (density, expansion coefficient α) and can be approximated with the help of the Simha-Boyle rule ($\Delta\alpha T_g$ = constant):[58] $k = K(T_{g1}/T_{g2})$. If $K = 1$, the well-known Fox relation[59] results in an idealised additivity (volume and free volume) condition of miscible polymer blends.

In this article, the index 1 in the G-T-equation in miscible blends with one T_g means PLA, and the index 2 means PHBV (the indices are changed in some literature, the polymer with the higher glass transition temperature is then indexed with '2'). Thus, a greater value than about 1.2 ($\sim T_{g1}/T_{g2} = \sim T_{g,PLA}/T_{g,PHBV}$) indicates a miscible behaviour with a higher free volume than predicted by the Fox equation, which results in a lower T_g than predicted by the Fox equation. If two T_g were mentioned in the literature, and hence two phases were present, the number in row 9 in Table 2 accounts for the *k*-value of the G-T-equation using the higher glass transition temperature (here: 'PLA-like' glass-transition), and the indices are as mentioned above (w_1 = PLA). The number in row 10 in Table 2 accounts for the *k*-value of the G-T-equation for the glass transition at lower temperature (here: 'PHBV-like' glass-transition) with index 1 in the G-T-equation now meaning PHBV, and the index 2 meaning PLA. A greater value than about ~ 0.83 ($\sim T_{g1}/T_{g,2} = \sim T_{g,PHBV}/T_{g,PLA}$) indicates a miscible behaviour with a lower free volume than predicted by the Fox equation, which results in an higher glass transition temperature than predicted. Figure 3 illustrates the context by showing a symmetrical behaviour as shown by Schneider, Di Marzio.[57]

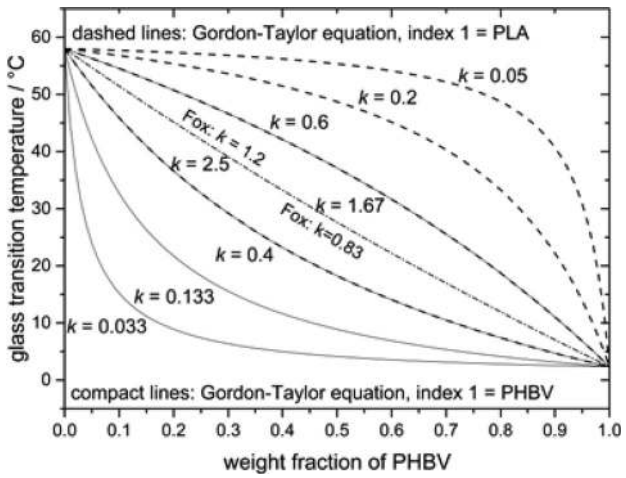

Fig. 3 – *Gordon-Taylor equation for PLA (T_g = 58 °C) and PBHV (T_g = 2.5 °C) with index 1 for PLA (dashed lines) or PHBV (full lines) and different k-values*

In miscible blends, the calculated *k*-value should be in the range of the *k*-value for reproducing the Fox equation (s. equation 6). Another value indicates interactions due to non-ideal mixing contributions. Taking the polymer with the higher glass transition temperature as 'index 1 polymer' in the G-T-equation, a higher *k*-value (here >1.2) indicates a softening effect of polymer 2 higher than expected. Taking the polymer with the lower glass transition temperature as 'index 1 polymer', a higher *k*-value (here >0.83) means that the hardening effect of polymer 2 is higher than expected. Low *k*-values indicate no or less change in the free volume of the polymer, which is indexed with 1 in the G-T-equation, having a nearly unchanged glass transition temperature. In immiscible blends with two glass transition temperatures, each glass transition can be analysed separately defining the right index. Nevertheless, miscibility over the whole composition range is not often given in the range of equal compositions due to thermodynamics (Figure 1) as example. A spinodal induced phase separation should lead to phases with inverted compositions, and the glass transition temperatures can be calculated for each phase with the G-T-equation, with the matrix phase indexed as phase 1. The *k*-values should then be related by $k_{1=PLA} \cdot k_{1=PHBV} = 1$. Deviation from one indicates different interactions in the phases.

Analysing the data in Table 2, it can be seen clearly that the 'PHBV-like' glass transition temperature indicates less miscibility than the 'PLA-like' glass transition temperatures. As an example, the *k*-values for the miscible blends (data taken from the experiments of Koyama, Doi[30]) are always around 2, by blending low molecular weight PLA (<12 kDa) in PHB, indicating a higher free volume than expected and good miscibility. When the molecular weight of PLA is increased to about 12 kDa, the k-value for fitting the higher glass-transition

Table 2 – *Summarized data from literature concerning miscibility of PLA / PHB blends*

PLA			PHB/PHBV			$\delta_1 - \delta_2$		Gordon-Taylor-Parameter		Temperature/°C	Miscibility	Remarks	Reference
type	M_n	M_w	type	M_n	M_w	this work	lit.	calc.[a]	lit.				
	[10^3 kDa]			[10^3 kDa]									
L	52	99	n.s.	169	425	>0.35				200	i	Quenching 100 K min^{-1} ; Lapol additive	15
L	87	114	RS	100	n.s.	>0.32				190	i/p	Quenching not mentioned; slight decrease in T_c and nearly no decrease in T_m of PLA; T_g of PLA around 48 °C for mixtures with 10–20 % PHB	16
L	1.8		bac	222	794	<1.25	0.8			190	m	Whole range; interpenetrated spherulites; T_m (PHB) = f(wPLA); calculated difference of solubility parameter	17
L	159	417				>0.23					i		
L	n.s	11	R		500	<0.79		2.3	0.43	230	m	Quenching lq. N_2, mixture 1:1 of L and D PLA, assumption D = 2; low molecular weight polymer enhance miscibility	18
D	95	124				>0.27							
DL	44 (M_v?)		n.s.	50 (M_w?)		<0.46					m	Assumption 200 °C	19
L	140 (M_v)		RS	31	34	<0.45		1.45	0.7	220	m	Melt quenching; from melting point depression of PLA: χ = –0.12; a-PHB induces banded-PLA spherulites; assuming $M_v M_n^{-1}$= 1.5	28
DL	44	79	RS	13	13	<0.69		1.7	0.6	220	m	Melt quenching	22
L	n.s.	100	V12	n.s	n.s.					200	i	No T_m variation	21
L	83	150	n.s.	272	600	>0.22		0.009		190	i	Cooling 20 K min^{-1}; T_c (PLA) shift indicates dispersion of small amounts of PLA in PHB	24
			H12	266	638								
DL	242 (M_v)		H11	n.s	n.s.					200	i	Rapidly quenched to –60 °C	25
	n.s	n.s.	V	n.s	n.s.	>0.36		~0.02		200	i	Cooling 10 K min^{-1}; no T_m variation; fine dispersion (0.4 μm) by low PHBV content; PLA: Nature Works 3051D (assuming M_n = 60 kD for injection molding type) PHBV: Tianan Enmat Y1000P (M_n ~92 kD (own measurement))	27
L	n.s	220	n.s	n.s.	230	>0.3				200	i*	Assuming D = 2, *Tg variation 61–63 °C for PLA; x-ray and FT-IR: immisc; discussing miscibility as a function of T_{cc}: one T_{cc} misc.: 25/75 or 75/25, two T_{cc} immisc.: 50/50	20
L	n.s	200	n.s	295	600	>0.25				200	i	Melt quenched; assuming D = 2; low M_w PHB: T_m, T_{cc} variation as function of low M_w-PHB amount	54
			n.s	5		<0.86		1.2			p		
L	n.s	n.s.	V20	n.s	n.s.			0.016	88	200	i	Cooling 10 K min^{-1}; DMA: decreasing activation energy and relaxation times confirm with enlargement of T_g transition: molecular interactions; small effect on T_m equilibrium of PLA; low molecular weight interphases / dispersion of PLA in PHBV	45
L	456	684	RS	67	94	>0.27		0.095		200	i	Quenched to –50 °C; AFM: surface area homogeneous by 5 kDa PHB, phase separated morphology by 16 and 67 kD with finer domains in the 16 kDa PHB blend; 16 kDa misc. up to 25 % PHB; 5 kDa misc. up to 50 % PHB; no T_m variation (PLA) with 67 kDa and 16 kDa PHB, strong influence on T_c with 5 kDa PHB	26
				16	19	>0.47		0.8			p		
				5	8.5	<0.77		10			p		
DL	17	36	R	300	650	>0.47		0.4–0.5		200	p	Rapidly quenched to –100 °C, PLA-Co-Caprolacton shows miscibility at M_n ~18 kD and 30–60 % Caprolacton	29
L	294	530	R	300	650	>0.18			0.002	200	i	Rapidly quenched to –100 °C; two glass transitions if M_w > 20 kD, slight dependence of T_g by M_w between 20–39 kDa indicating some partial miscibility; one T_{cc} in miscible blends with increasing temperature by increasing PLA weight fraction, two T_{cc} in immiscible blends with great separation; two T_{cc} in partially miscible with lower separation; M_w for calculation of solubility parameter difference (remark: not reproducible 0.34 typing error?)	30
methanolysis	50	80				>0.31			0.04		i		
	23	39				>0.42		0.6	0.03		i/p		
	19	34				>0.45		0.2	0.07		i/p		
	14	20				>0.51		0.5	0.07		p		
	12	18				~0.54	0.34	2.0	0.4		m		
	8.9	16				<0.62		2.0	0.5		m		
	7.7	13				<0.66		1.8	0.6		m		
	4.5	9.9				<0.83		2.0	0.5		m		

PLA			PHB/PHBV			$\delta_1 - \delta_2$		Gordon-Taylor-Parameter		Temperature/°C	Miscibility	Remarks	Reference
type	M_n	M_w	type	M_n	M_w	this work	lit.	calc.[a]	lit.				
	[10^3 kDa]			[10^3 kDa]									
L(4)	110	187	V40	170	425	>0.27		0.034		170	i	Cooling to –30 °C; fine dispersion of PHBV (domain size: 0.3 µm) in PLA at 10 w% PHBV, at 30 w% PHBV 2 µm domain size; nearly no variation of T_m (PLA), nearly no variation of T_{cc} except 10 w% PHBV; PLA: Nature Works 2002D; PHBV: Tianan Enmat Y100P	31
L(4)	n.s	160		n.s	280	>0.31					i	Cooling to –20 °C; some compatibility because DT_g = 8 °C; PLA: Nature Works 3051 D (Inj. Mold.), 4042 D (Films), 6202 D (fibers), PHBV: Tianan; assuming D = 2	32
L(8)	n.s	200	V5			>0.29				200	i		
L(2)	n.s	140				>0.32					i		
L	n.s	n.s.	V	n.s	n.s.			0.18	0.2	175	i/p*	Cooling to –20 °C; 10 K min^{-1}; T_m PHBV = 152 °C, *low miscibility stated	33
L	110	253	bac., thermal degradat.	83	166	>0.32		0.07	0	200	i	Rapidly quenched 50 K min^{-1}; PHB 14 kDa: misc. up to 80/20, PHB 7.4 kDa: misc. up to 80/20, PHB 4 kDa: misc. up to 60/40; miscibility depends on mol. weight and blending ratio; higher crystallization rate of PLA with low molecular weight PHB; PHB: from bacterial PHB by thermal degradation; Nature Works Type of PLA	34
				14	26	~0.57		1.1	0.02		p		
				7.4	14	<0.71		1.3	0.08		p		
				4	8.4	<0.93		1.4	0.08		p		
L	338	778	RS	93	140	>0.25		0.11	0	200	i	Quenched at –100 °C; misc. strongly dependent on mol. weight: 17.5 kDa: misc. up to 85/15 %, 5.9 kDa: misc. up to 50/50 PLA/PHB,; T_{cc} decrease remarkably with low mol. weight PHB; PHB is trapped in PLA spherulites; crystal. blends (120 °C) of PLA/PHB (5.9 kDa) shows phase separation in the amorph.phase	35
				18	21	>0.46		1.13	0.08		p		
				5.9	9.4	<0.73	0.58	1.9	0.34	1.9	p		
L	219	350	bac	227	590	>0.21				200	i	Rapidly cooled to –50 °C	36
				3120	5300	>0.13					i		
DL/L	3.3	n.s.	nat.	2.2	n.s.	<1.9		1				Rapidly quenched, PHB-PLA-Blockcopolymer misc.; phase separation by annealing at 65 °C, assuming 190 °C	37
n.s	n.s	n.s.	bac	n.s	n.s.			0.02		210	i	lq. N_2 quenching; no T_m variation; better dispersion with epoxidized side chain PHA	38
DL	n.s	n.s	bac	87	230			2.2–2.7	0.03			T_g(DL-PLA) = 45 °C, modulated-DSC; for 25% PHB	39
L	190	n.s	n.s	n.s	470	>0.21				190	i	Quenched to –100 °C, assuming D = 2	40
	56	n.s				>0.31					i		
	12	n.s				<0.55		~1.5			m		
	5.8	n.s				<0.75					m		
n.s	n.s	n.s	V	n.s	n.s			0.02	0.05	200	i	Rapidly quenched to –40 °C; slight T_c and T_m (PHBV) variation; PLA: Nature Works 7001 D; PHBV Tianan Enmat Y1000P	13
DL-PEG	n.s	n.s	bac	n.s	n.s.						i	Internal compatibilisation by PEG-Copolymer; PLA-22600-PEG-4000	41
	27	n.s	n.s	n.s	n.s.			~0.6			m		
DL	43	82	bac	300 (M_v)		>0.35				200	i	Rapidly cooled to –60 °C; assuming $M_v M_n^{-1}$ = 1.5; melt blending implies greater miscibility than precipitation of solvent mixture	42
L	83	150	bac	n.s	600	>0.21					i	Potential interaction in the immiscible blends by IR; * assuming D = 2 and room temperature	43
	3.3	4.3				<0.75					m		
L(4)	n.s	n.s	V	n.s	n.s			~0.15				Cooling to 25 °C; 10 K min^{-1}; ~ from Fig. 9b.	44

n.s.: not specified; a: see text; b: L(2) = L-Lactid with 2 % D-Lactid; V20 = 20 % Valerat in PHBV; H = Hexanoat; R (S) = configuration of PHB; bac.= bacterial; nat.= natural; when M_n was given a dispersion D = 2 was assumed

temperature ('PLA-like') drops below 1, indicating less miscibility but due to the magnitude (0.6–0.2) of the *k*-value, remarkable interactions between PLA and PHB should be present leading to a shift in the glass transition temperature. Partial miscibility that changes to immiscibility can therefore be claimed. In contrast, the *k*-values of the lower temperature glass transition ('PHB-like') are often nearly independent of composition and are below 0.1, indicating lower interaction and immiscibility.

From an application point of view, a low molecular weight component in a polymer blend is not often used because polymers with low molecular weights often do not exhibit targeted properties, especially not high strength. Low molecular weight components in a polymer mixture are often oligomeric plasticizers or in general additives. In practice, for an extrusion application, molecular weights of PLA and PHB or PHB-Copolymers of about 100 kDa (M_n), due to melt strength properties, are used, but for injection moulding applications, lower molecular weights than 100 kDa (M_n, e.q. 60 kDa) are possible for processing.

Therefore, for this study, we decided to examine the miscibility using nearly the same molecular weights in the range of 10–40 kDa (M_n).

Part I

Miscibility study with low to medium weight PLA and PHBV by Differential Scanning Calorimetry (DSC)

The glass transition temperature (T_g), crystallisation and cold crystallisation peak temperature (T_c, T_{cc}), melting temperature (T_m), and enthalpy of fusion, crystallization and post crystallisation (ΔH_m, ΔH_c and ΔH_{cc}) of binary blends of PLA and PHBV in varying ratios were determined from the DSC thermograms, and are summarized in Table 3. Due to the general shape of the free mixing enthalpy curve, derived by Flory and Huggins, which predict less miscibility at equal parts and better miscibility with a major phase (Equation 1, Figure 1), three weight ratios of PLA to PHBV were used: 80:20, 50:50 and 20:80 weight percent. As densities are equal[43], weight fractions are volume fractions.

PLA-rich blends

Figure 4a and b shows the thermograms of the first heating scan after quenching the samples from 190 °C with liquid nitrogen to obtain amorphous structures, and Figure 4c and d shows the heating scan after controlled cooling from the melt with 10 K min^{-1}, for the 80:20 blend of PLA and PHBV.

According to these thermograms, the glass transition temperature, cold crystallization peak temperature, and melting peak temperature show clear trends. Post crystallization and melting enthalpies are nearly equal, indicating the presence of an amorphous phase after quenching.

No cold crystallization peaks of pure PHBV or PLA phases can be seen in Figure 4a, b (high M_n PHBV ~37° C, methanolysed PHBV 15/20 kDa: 33–36 °C; high M_n PLA: 125–130 °C, hydrolysed PLA 15/20 kDa 100–120 °C; own measurements). Hence, no pure PHBV and PLA phases are present. Therefore, a broad cold crystallization region with shaped peaks (shoulders) in the region between he cold crystallization temperatures of the pure components are clearly visible, indicating interactions between PLA and PHBV. Quenched samples show only one glass transition temperature, thus miscibility in the molten state at 190 °C is given.

In the samples with controlled cooling (Figure 4c-d), the shaping is more intense and the range of cold crystallisation is broadened for samples up to 30 kDa molecular weights. Heat capacity change at the glass transition (ΔC_p) is low for samples with low molecular weight and ΔH_c, in the cooling scan is high for samples with low molecular weights (see Table 3). The amorphous amount in the blend after controlled cooling is low in samples with low molecular weights. This may be due to the higher mobility of low molecular weight chains, which allows a faster crystallisation. Due to only one glass transition, the crystallization in the cooling scan should therefore take place from a homogenous melt. The T_g in the quenched and control-cooled samples reveals that the crystallisation does not change composition to a great extent. This is somewhat surprising since two crystallization temperatures can be seen in the cooling scan (Table 3). Miscibility should also be given in the amorphous phase after crystallisation. Nevertheless, comparing the post crystallisation range in the quenched and in the control-cooled samples, deviations in post crystallization pattern indicate deviations in the morphology of the amorphous phases. So, although miscibility in the amorphous state in the control-cooled sample is postulated, the existence of a less homogeneous phase after controlled cooling may also be postulated. We interpret this behaviour as molecular fluctuations which are forced by the 'thermodynamic push' of potential crystallisation enthalpy – which is not outperformed by enthalpy of mixing, leading to separations in the submicron scale. In few cases, a glass transition point with a very low intensity of a PHBV-rich phase is found at about 10 °C (Table 3). These phases may be the result of the above-mentioned fluctuations.

The cold crystallization temperature of the samples exhibit a general trend to a higher tempera-

Table 3 – *Thermochemical data of PLA/PHBV blends with low molecular weight*

M_n [kDa] PLA/PHBV	PLA [w%]	T_g Fox*	Heating				Cool.	Heating				Cooling	Heating		Heating		Cool.	Heating	
			T_g [°C]	ΔCp [J(g K)$^{-1}$]	T_g [°C]	ΔCp [J(g K)$^{-1}$]	T_g [°C]	T_{cc} [°C]				T_c [°C]	T_m [°C]		ΔH_{cc} [J g^{-1}]		ΔH_c [J g^{-1}]	ΔH_m [J g^{-1}]	
			quenching		controlled cooling			quenching		cc			quench.	controlled cooling	quench.	cc		qu.	cc
7.5/10	80	38	34	0.46	34	0.06		90		73 95		75 92	132 148	134 148	44	11	38	44	49
	50	20	11 23	0.32 0.09	47	0.14	44	63 99		96		94	148 155	141 153	30 16	10	44	63	59
	20	4	3	0.55	9 48	0.01 0.02	42	46 85br		85br		102	137 156	146 156	44 1	5	68	77	80
19/10	80	41	33	0.48	36	0.23	32	88		76 98		77 90	124s 151	152	49	27	21	49	49
	50	21	10 24	0.27 0.08	48	0.17	41	63 98		96		93	127s 154	141 154	34 18	18	43	70	68
	20	4	2	0.48	4–10 50	0.01 0.03	45	48 83		90br		101	156	148 157	41 1	9	66	74	78
15/15	80	41	9 35	0.03 0.33	4 35	0.02 0.28	34	87 93		87 100		85	152	153	48	40	6	48	49
	50	23	6 25	0.19 0.03	–6–3 48	0.03 0.23	44	55 97		91		98	157	148 160	29 16	18	40	66	66
	20	7	–1	0.53	5 48	0.03 0.06	43	42 80br		88br		106	161	154 163	38 2	5	66	76	82
15/28	80	42	11 34	0.01 0.39	38	0.27	33	83 92		81 100		87	153 162	154 165	47	29	15	47	50
	50	24	7 28	0.26 0.05	49	0.14	46	54 63 101		90		101	151s 163	154 165	28 16	19	40	72	70
	20	9	1	0.47	69 51	0.02 0.02	47	46 79		87br		108	166	160 168	39 1	7	65	79	82
19/ 23.5	80	42	38	0.47	37	0.23	35	92 99sh		77s 100		91	153 163	153 160	50	27	19	50	52
	50	24	10 25	0.19 0.08	7–13 50	0.02 0.19	46	63 106		95		99	154s 163	153 163	29 13	14	39	63	63
	20	8	2	0.53	8–13 50	0.03 0.03	47	47 84br		88		106	166	159 168	37 1	6	62	75	79
27/ 23.5	80	43	39	0.41	37	0.35	33	92		89 102		88br	154 161	154 161	52	44	5	52	52
	50	25	9 26	0.19 0.16	3–10 49	0.02 0.22	52br	64 108		98		94	155 162	154 163	27 15	19	38	64	62
	20	9	2	0.49	3 52	0.03 0.03	51	46 82br		90		103	165	157 167	38 2	9	68	77	81
32/28	80	43	47	0.41	45	0.28	42	95		97		91	157 167	157 167	45	42	3	45	49
	50	25	3 dist.	0.26 dist.	1 51	0.1 0.19	47?	45 93 110		100 115		109	159 168	161 170	15 30	31	28	63	65
	20	9	1	0.40	3 52	0.08 0.08	50	44 79 98		90 102		105	168	162 169	32 8	9	70	76	81
35/ 33.5	80	44	44	0.41	48	0.40	46	94 105		103		95br	157 169	150158 170	46	43	1	48	49
	50	26	1 dist.	0.21 dist.	2 49	0.01 0.19	46?	42 96 110		103		107	159 169	159163 171	14 24	27	32	64	64
	20	10	1	0.33	4 55	0.05	51	42 87 106		105br		111	158 169	164 170	24 9	9	64	85	86
37.5/ 39.5	80	44	4 47	0.03 0.34	51	0.37	47	99		105		105br	158 171	149159 172	37	34	1	39	42
	50	26	0 dist.	0.23 dist.	0–8 49	0.03 0.16	47	46 101 111		106		109	158 169	159164 171	18 26	28	32	67	67
	20	10	3	0.44	4 54	0.02 0.09	49	46 91 116		107br		110	169	165 171	37 9	9	69	82	88

dist. = disturb by post crystallisation peak of PHBV phase; *glass transition calculated with the Fox equation using the Fox-Flory equation: $T_g = T_{g\infty} - K/M_n$ for calculating T_g of pure polymers and data of Jamshidi, Hyon[60] for PLA ($T_{g\infty}$ = 58 °C, K = 55000) and data for PHBV from own measurements with $T_{g\infty}$ = 2.5 °C and K = 87000; s = shoulder, br.= broad

ture, with a higher molecular weight indicating lower mobility of higher molecular weight fractions (Figure 4a, c). For most samples, there are two melting temperatures. These melting transitions are related to PLA and PHBV due to the shaped post-crystallization peak indicating two crystallizations, and ΔH_m. Assuming a crystallinity of about 35–40 % for PLA and 60–65 % for PHBV, ΔH_m should be in the range of 43 – 49 J g^{-1}. Melting exotherms at low temperatures (~130 °C) are associated with imperfectly crystallised PLA, due to interlamellar crystallization with PHBV.[17,29,32,34,35,41–43,45]

For a tentative quantification of miscibility, the G-T-equation (Equation 6) was applied with the constant k as a fitting parameter with molecular significance, as defined by Schneider.[56,57] The calculat-

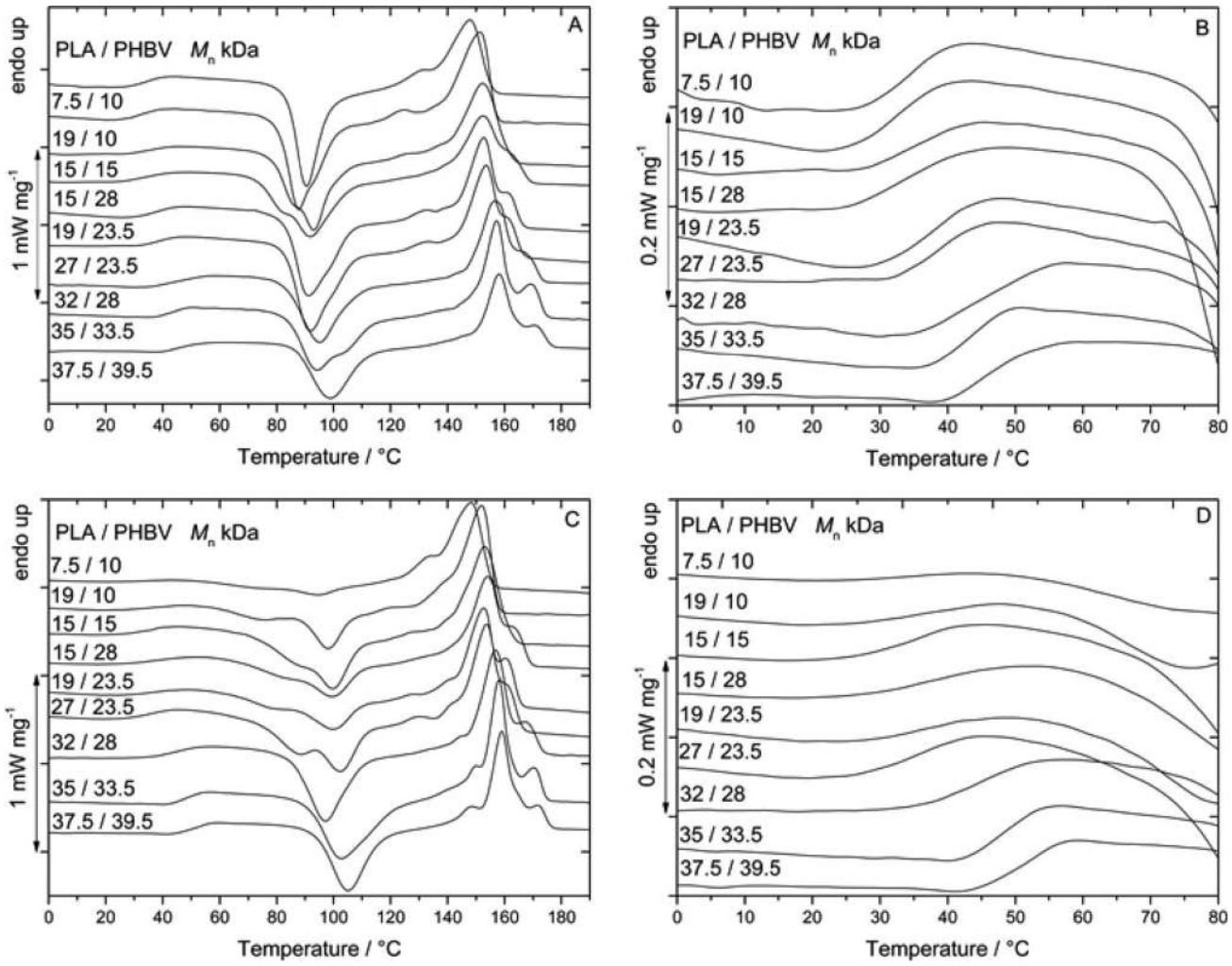

Fig. 4 – *DSC Thermograms of PLA / PHBV Blends (80:20), 4a and 4b: melt (190 °C) quenched samples (liquid nitrogen), 4c and 4d: samples with controlled cooling (20 K min^{-1}) from the melt; molecular weights are presented at the curves, which are shifted for better visualisation; double arrow indicates scale of heat flow.*

ed *k*-values in the range 0.8 to 2.5 (w_1 = PLA) are illustrated in Figure 5, assuming a composition of 80:20 (PLA:PHBV) in the amorphous phase of the control-cooled sample. (Otherwise, due to changes in composition during crystallization in the cooling scan, the composition has to be changed in some samples to about 83:17 using the same *k*-values for the quenched and the control-cooled sample.) The *k*-values indicate a change in quality of miscibility between the samples with molar weight of 27/23.5 and 32/28 kD, respectively. The *k*-values greater than 1.2 (w_1 = PLA) - expected by ideal miscibility due to Fox equation - can be interpreted in terms of an expanded free volume leading to lower glass transition temperatures in miscible blends. The *k*-values of miscible blends in the range of 2 confirm the data of Koyama, Doi[30] and Chang, Woo[18] for low molecular weight PLA blended in high molecular weight PHB (bacterial origin), and the data of Ohkoshi, Abe[35] for low molecular weight atactic PHB blended with high molecular weight PLA.

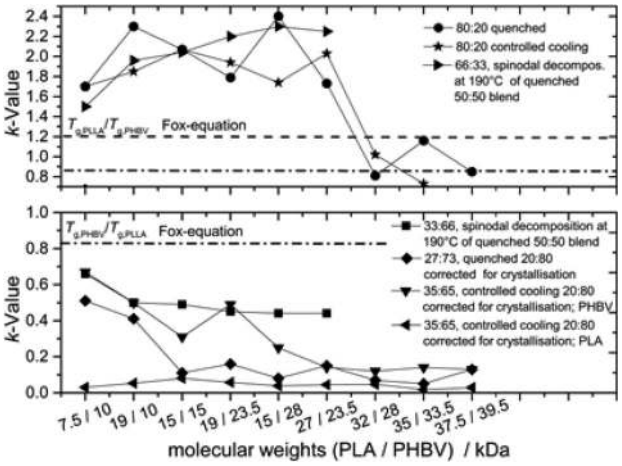

Fig. 5 – *k-Values derived from G-T-equation for 80:20, 50:50 and 20:80 blends of PLA and PHBV; (eq. 6; see also Fig. 3 for explanation); 80:20 control cooling with PLA/PHBV = 37.5/39.5: k = 0.5*

Data from Ni, Luo[34] for blends of low molecular weight PHB (bacterial origin) with high molecular weight PLA is considerably lower (Table 2).

PHBV-rich blends

Due to the symmetry of the Flory-Huggins equation, miscibility in the 80:20 blends should result in miscibility in the 20:80 blends of PLA and PHBV if density and molecular weights of the components are equal.

Figure 6a-d shows the thermogram of the 20:80 PLA:PHBV blends (data is included in Table 3). The results of the post-crystallisation and melting enthalpies in the quenched samples reveal that no pure amorphous structures are present in the quenched samples. Annealing the samples at ambient temperature after quenching for evaporation of the water film (condensate from air humidity on the cold crucible) induces therefore some crystallisation of PHBV. Own measurements with high molecular weight PHBV (Enmat Y 1000P) disclose a T_{cc} at 37 °C, (10 K min^{-1} heating rate, peak maximum), an onset temperature at 32 °C, and a starting post-crystallization at around 25 °C, as shown by the differentiated DSC curve. Barham, Keller even stated complications in T_g measurements by post-crystallization of PHB whenever it is heated above 10 °C.[61] Taking into account that the 'missed' post-crystallisation enthalpy belongs to crystallised PHBV, the calculation (Equation 7) of an amorphous composition of PLA:PHBV of about 27:73 for all samples, except the 35/33.5 kDa sample, is possible (35/33.5 sample 31 : 66) using 146 J g^{-1} as melting enthalpy for PHB.[61]

$$w_{PLA} = \frac{0.2}{0.2+z}; \quad z = 0.8 \cdot \left(1 - \frac{\left(\Delta H_m - \Delta H_{cc}\right)}{0.8 \cdot 146}\right) \quad (7)$$

Only one post-crystallisation peak with relevant intensity is detected at around 45 °C (Figure 6a), indicating a nearly undisturbed crystallising PHBV phase compared to the post-crystallisation temperature of pure PHBV (37 °C), and 80 to 90 °C in the PLA-rich 80:20 blends. Post-crystallization peaks just above the noise level at about ~ 80–85 °C

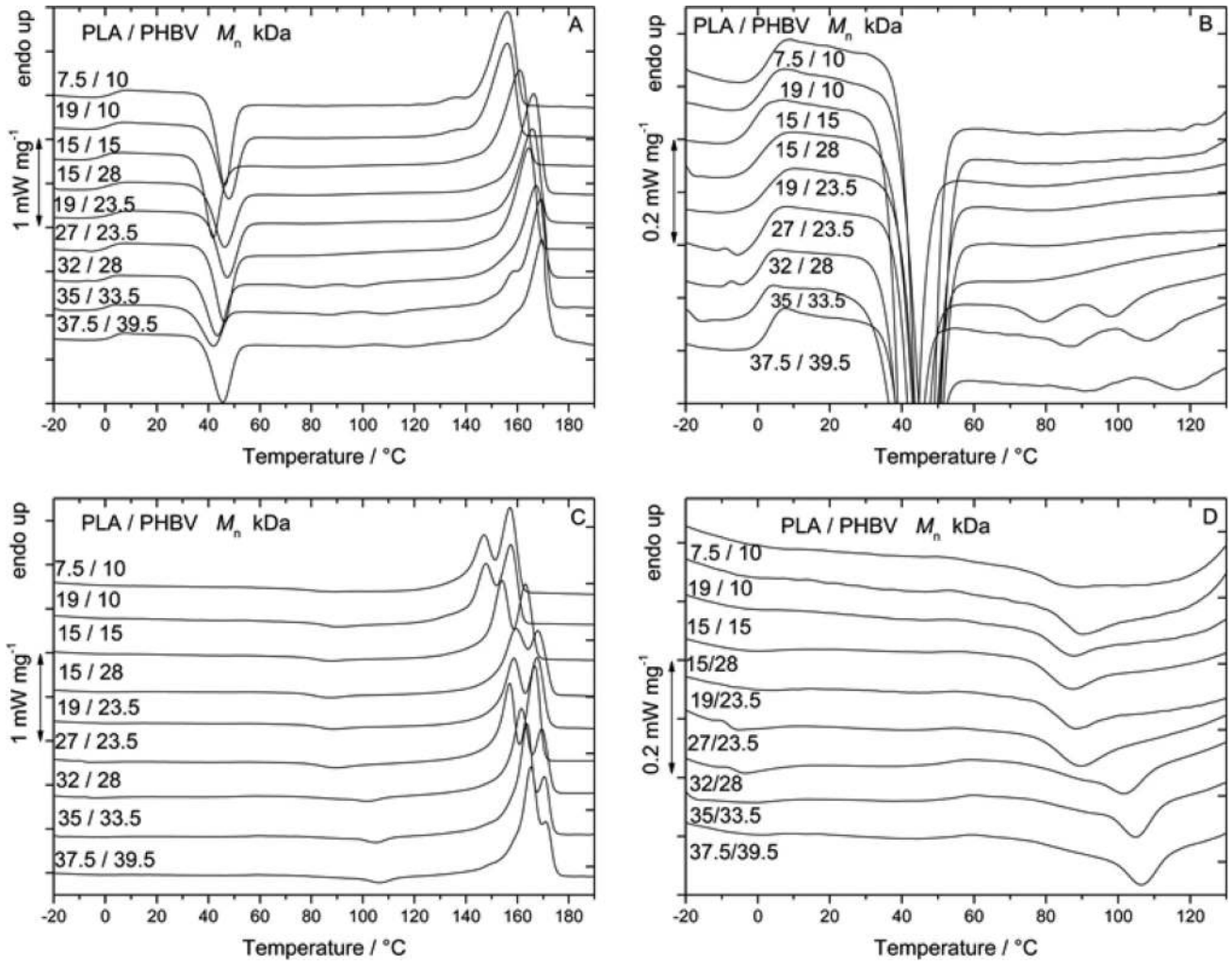

Fig. 6 – *DSC Thermograms of PLA : PHBV Blends (20:80), 6a and 6b: melt (190 °C) quenched samples (liquid nitrogen), 6c and 6d: samples with controlled cooling (20 K min^{-1}) from the melt; molecular weights (kDa) are presented at the curves, which are shifted for better visualisation; double arrow indicates scale of heat flow*

can tentatively be evaluated for blend compositions up to 30 kDa, which may belong to phases enriched with PLA, due to PHBV post-crystallization or to miscible phases. Due to the low intensity of this peaks, amounts of PLA may be trapped in the interlamellar regions of PHBV spherulites, as stated by several authors.[17,29,32,34,35,41–43,45] For the higher molecular weight blends, two more pronounced post-crystallisation peaks emerge in the thermograms. These post-crystallisations may belong to phases enriched with PLA as mentioned above. The almost pure PLA phases, due to post-crystallization temperature – especially for the blend with the highest molecular weight (116 °C, Table 3), indicate a change in phase morphology at molecular weights above ~ 30 kDa. Only one glass transition occurs in the quenched sample at around 1–3 °C, due to the post-crystallisation peak of PHBV, covering potential glass transitions in higher temperature ranges. The distinct intensity of the heat capacity change (Table 3) indicates the existence of great amounts of this low T_g amorphous phase. In the second heating scan (with controlled cooling before), two glass transition regions with a lower intensity due to crystallisation of great amounts of matrix polymers in the cooling step (Table 3) occur in most samples. Owing to this crystallisation, no post-crystallisation peak of PHBV emerges in the heating scan after controlled cooling. Less intense post-crystallisation peaks of phases enriched with PLA and nearly pure PLA phases, due to immiscibility especially in the blend with the highest molecular weight as mentioned above, can therefore be seen in the second heating scan.

Therefore, it can be concluded that symmetrical behaviour of PLA:PHBV 80:20 and 20:80 blends concerning miscibility, due to thermodynamic reasons, is neutralized by the well-known high crystallisation rate of PHB and PHB-copolyesters.[21,62] The different post-crystallisation behaviour of samples with molecular weights higher than 30 kDa remind of the above mentioned change in the magnitude of the *k*-value in 80:20 blends. Analysing the glass transition in the quenched samples at about 0 °C by calculating the *k*-value of the G-T-equation using the corrected composition data (27:73; s.a.), values around 0.5 to 0.05 can be calculated (w_1 = PHBV, Figure 5). This indicates miscibility for blends with the lowest molecular weights in the melt (<10–15 kDa) due to the relation of the *k*-values based on w_1 = PLA or PHBV (see Figure 3: $2 \cdot 0.5 = 1$). Partial miscibility to immiscibility for blends with molecular weights higher than ~ 15 kDa can be concluded by the declining *k*-value. This behaviour also contradicts the assumed symmetrical behaviour of PLA:PHBV blends with a composition of 20:80 or 80:20. From a thermodynamic point of view, an additional force for phase separation in the 20:80 PLA:PHBV blends should be present in contrast to the 80:20 blends. This force might be the intermolecular interaction (hydrogen bonding) between the C=O group and the CH_3 group, combining two helical structures in PHB (and P(HB-co-HH_x)) postulated by Sato.[63,64] These inter- and intra-chain interactions can be active only in blend compositions where, despite miscibility, the interacting polymer segments are not surrounded by polymer segments of the second blend component. Therefore, the interactions between the two polymers in the 20:80 blends are not only reduced because these interactions lead to a higher plasticising effect of PHBV on PLA or a lower hardening effect of PLA on PHBV (due to a greater free volume) than expected. Reduced interaction should lead in miscible blends to higher *k*-values based on index 1 = PHBV, indicating only a loss in free volume in comparison to the 80:20 blends. The dropping *k*-value therefore indicates a starting immiscibility in the 20:80 blend with molecular weights greater than ~ 15 kDa.

The analysis of the glass transition temperatures in the control-cooled samples with crystallisation during the cooling step gives additional information: Assuming that the measured crystallisation enthalpy belongs mainly to PHBV, because no post-crystallisation peak of PHBV and a post-crystallisation peak of mainly PLA can be seen in the subsequent heating scan, and due to higher crystallisation rate and crystallinity in pure PHBV, a crystallinity of about 56–57 % for PHBV and of about 0–6 % for PLA can be simulated. This would change the overall composition in the amorphous state from 20:80 to 37:63–34:66 ~ 35:65.

$$w_{PLA} = \frac{0.2 \cdot (1 - x_{c,PLA})}{0.2 \cdot (1 - x_{c,PLA}) + 0.8 \cdot (1 - x_{c,PHBV})}; \quad (8)$$

$$x_{c,PLA/PHBV} : \textit{crystallinity of PLA or PHBV}$$

Using this composition for calculating the T_g in the second heating scan, *k*-values of about 0.67 to 0.1 (w_1 = PHBV, Figure 5) result for the lower temperatures T_g indicating miscibility in the amorphous PHBV-rich phase of low molecular weight blends (< 10–15 kDa), as shown above for the quenched sample. The broadness of the glass transitions of the samples with molecular weights of 19/10 and 19/23.5, respectively, can be explained on the one hand by variations in composition (rather more amorphous PHBV than more PLA), or on the other hand by a dependence of the T_g of the molecular weight distribution in the real phases, which may be different. The simulation of those T_g with a composition of 35:65 for PLA / PHBV leads to a variation of the *k*-value indicating miscibility (>0.6) or beginning immiscibility (~0.36). The analysis of the

higher glass transition temperature results in *k*-values of around 0.05 (w_1 = PLA, Figure 5) taking the above-mentioned composition into account. This indicates a more or less pure PLA phase. Therefore, due to the reduction of PHBV in the amorphous phases during crystallisation in the control-cooled samples, phases with high amounts of PLA should be formed.

For low molecular weight blends (< 30 kDa), one melting transition occurs in the quenched samples belonging to post-crystallised PHBV, as no distinct post-crystallisation of PLA can be detected (Table 3: max 1 J g^{-1}). A shift in melting temperature may be caused by a higher mobility of chains (higher free volume) based on the low molecular weight and less perfect crystals. Due to post-crystallisation of PLA, shoulders can be seen in higher molecular weight blends > 30 kDa. In the control-cooled samples, two melting transitions can be seen. The intensities of the blends with molecular weights lower or higher than 30 kDa are inverted. No melting transitions below 160 °C, which refer to the applied PLA-type, can be detected for the higher molecular weight blends (> 30 kDa). The intensity of the first melting transition is quite strong, assuming a lower melting enthalpy and a lower crystallinity for PLA compared to PHBV (93.5 J g^{-1} [65] which is ~ 64 % of PHBV[61]). The expectation for a 20:80 blend of PLA and PHBV is an intensity relation of 1:6.3 (equal crystallinity) up to 1:10 (assuming 40 % and 65 % crystallinity). Hence, it can be assumed that the first melting transition belongs to crystallised phases made of interpenetrating spherulites or PHBV spherulites disturbed by included amorphous PLA or interlamellar post-crystallised PLA, as discussed by several authors.[17,29,32,34,35,41–43,45] The higher melting point transition should therefore belong to a pure PHBV phase.

50:50 blends

Figure 7a and b shows the thermograms of the quenched samples for a 50:50 blend of PLA and

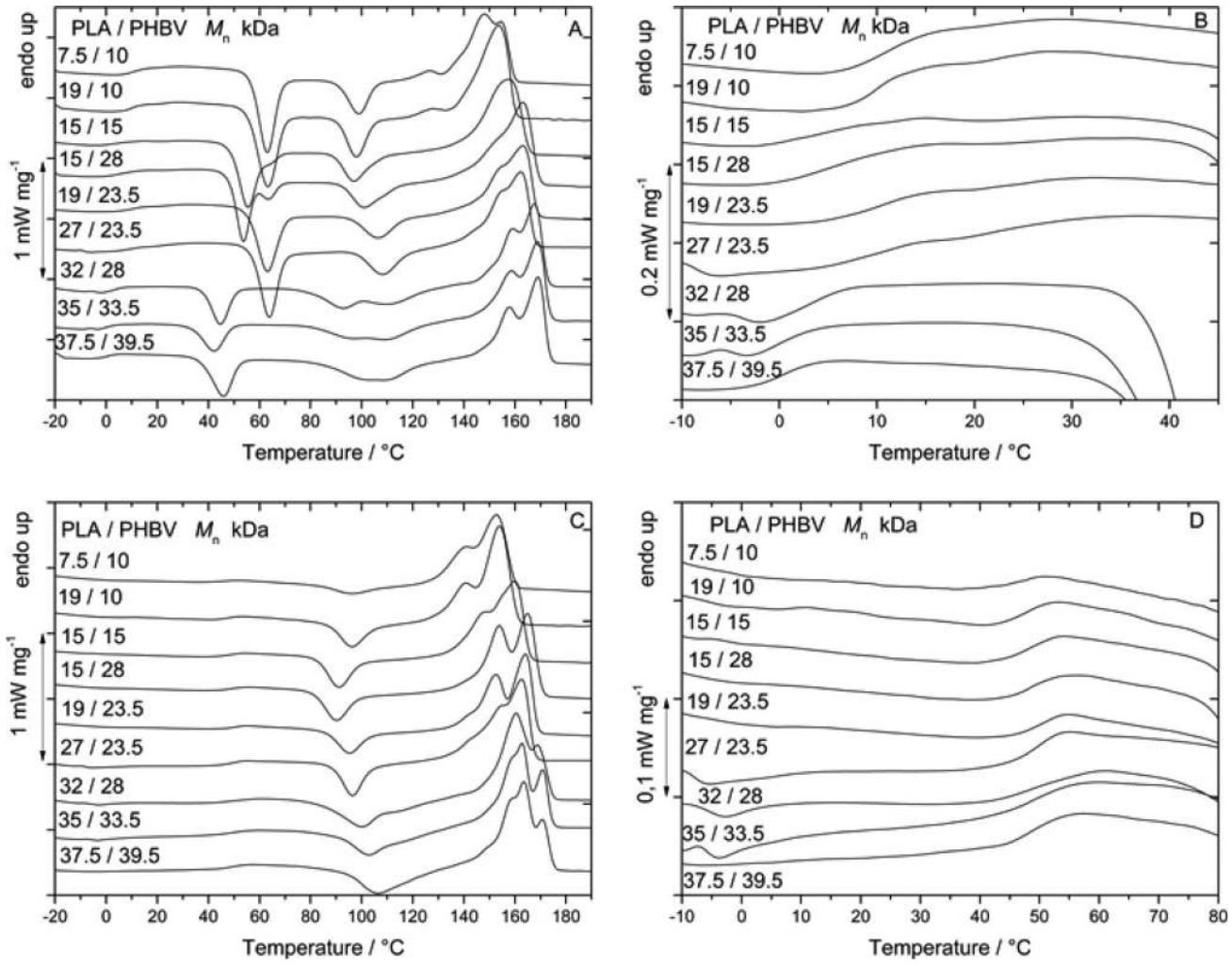

Fig. 7 – *DSC Thermograms of PLA : PHBV Blends (50:50), 7a and 7: melt (190 °C) quenched samples (liquid nitrogen), 7c and 7d: samples with controlled cooling (20 K min^{-1}) from the melt; molecular weights (kDa) are presented at the curves which are shifted for better visualisation; double arrow indicates scale of heat flow*

PHBV. Samples with molecular weights higher than ~ 30 kDa can be distinguished from samples with molecular weights less than ~ 30 kDa: The thermograms of the first group show one glass transition temperature, a first post-crystallization temperature between ~ 40–50 °C (which potentially covers the second glass transition temperature), and a second post-crystallisation range with two peaks at 90–100 °C and around 110 °C. Enthalpies of post-crystallisation at 90–100 °C are higher than those at 40–50 °C. Post-crystallisation temperatures at 40–50 °C and about 90 °C are also detected for the post-crystallisation of PHBV in the 20:80 blends, and for the post-crystallisation of PLA in the 80:20 blends (Table 3). Therefore, for samples with molecular weight above > 30 kDa, a phase separation due to immiscibility of the PLA and PHBV phase in the liquid state at 190 °C can be assumed. Nevertheless, a third phase, with a T_{cc} around 110 °C, also exists which should belong to nearly pure PLA phases.

Contrary to samples with molecular weights above ~ 30 kDa, samples with molecular weights below 30 kDa exhibit two glass transitions, a first post-crystallisation temperature between ~ 50–60 °C, and a second post-crystallisation temperature between ~ 100–110 °C, with the first post-crystallisation enthalpy being higher than the second. The two glass transitions in samples with M_n < 30 kDa indicate immiscibility at first glance: Taking the miscibility results of 80/20 blends of PLA and PHBV into account (changing miscibility between the samples with molecular weights of 27/23.5 and 28/32 kDa for quenched and control-cooled samples, respectively), the free enthalpy of mixture can tentatively be simulated by equation 2 using a solubility parameter difference of 0.65 $J^{0.5}$ $cm^{-1.5}$. Densities can be approximated with ~ 1.15 g cm^{-3} at 190 °C (melt) or ~ 1.2 g cm^{-3} in the "frozen solid state" during the cooling scan at ~ 100 °C, using ~ 5 · 10^{-4} as volume expansion coefficient for amorphous polymers.[50] Figure 8a shows the free enthalpy of mixture, from which miscible blends at 190 °C for blends with 20 % (v/v) PHBV up to a molecular weight composition of 27/23.5 kDa and less miscible to immiscible blends with molecular weights higher than ~ 30 kDa, can be postulated. For the blend with 32/28 kDa composition, spinodal decomposition can occur at 190 °C due to negative free mixing enthalpy but beginning convex curve of the spinodal (2nd derivative of eq.2 = 0 at ~ 23 % (v/v) PHBV). At 100 °C, miscibility is given for blend with 20 % (v/v) PHBV up to a molecular weight composition of 27/23.5 kDa. Immiscibility occurs for blends with molecular weights composition higher than ~ 32/28 kDa. Figure 8a shows also that, for a 50:50 (v/v) blend, spinodal decomposition occurs with a molecular weight composition of > 27/23.5 kDa, due to the curvature of the spinodal at 190 °C. The variation of the spinodal due to changes in solubility parameter difference is shown in Figure 8b, indicating high sensitivity for samples with molecular weights 15–30 kDa to variations. The two glass transitions in the thermograms of the quenched sample with 50/50 composition can therefore be explained with spinodal decomposition.

Analysing the post-crystallisation and melting enthalpies in the quenched samples reveals that not only amorphous phases are present in the quenched samples. Considering that the 'missed' post-crystallisation enthalpy belongs to crystallised PHBV, a

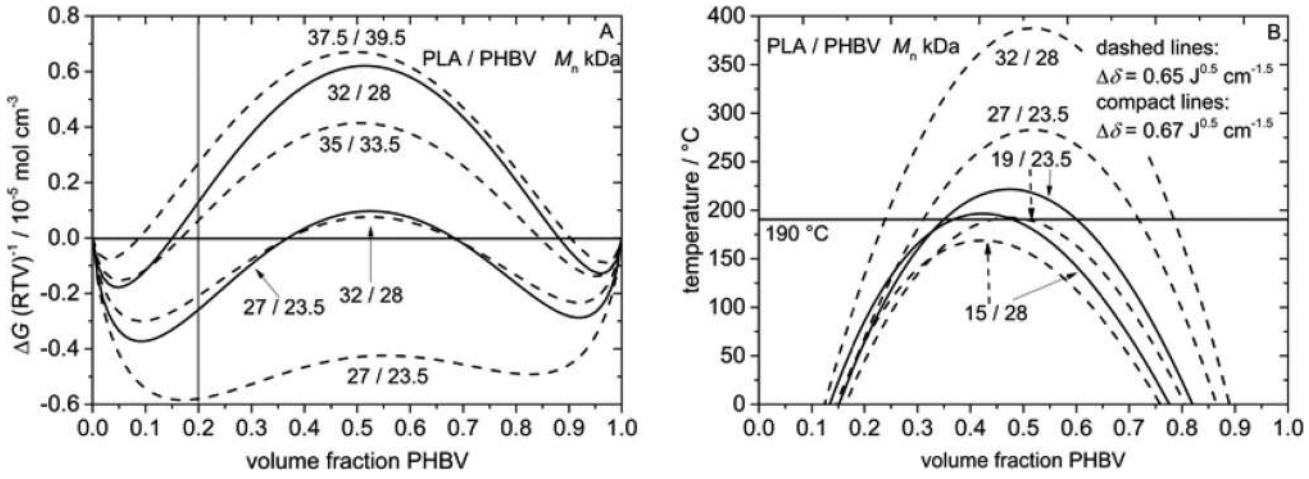

Fig. 8 – *Free enthalpy of mixing of PLA and PHBV according to Flory-Huggins theory and a difference in solubility parameter of 0.65 $J^{0.5}$ $cm^{-1.5}$ in dependence of molecular weight and temperature showing miscibility and immiscibility for blends with 20 % (v/v) of PHBV (vertical line), and spinodal decomposition for blends with 50 % (v/v) PHBV and molecular weights below ~ 30 kDa: dashed lines = 190 °C (quenching temperature), compact lines = 100 °C (assumed immobilization temperature in the cooling scan of DSC); density of 1.15 g cm^{-3} at 190 °C and 1.2 g cm^{-3} at 100 °C was assumed; b: spinodal curves for PLA PHBV blends according to Flory-Huggins Theory showing the sensitivity for spinodal decomposition by varying of the difference of solubility parameter; density = 1.15 g cm^{-3}*

calculation of an amorphous composition of PLA to PHBV results in a ratio of about 58:42 for all samples – except the 15/28 kDa sample (this sample has a ratio of 61:39). Analysing the glass transition temperatures of the spinodal decomposed phases with the G-T-equation, our results show that all glass transitions for samples with molecular weights below 28 kDa can be fitted with a *k*-value in the range of 2 (w_1 = PLA) or 0.5 (w_1 = PHBV), respectively (Figure 5). Thus, we assume a composition in the range of 66.6 PLA 33.3 PHBV in the PLA-rich phase, and 66.6 PHBV 33.3 PLA in the PHBV-rich phase.

The melting transitions of the quenched samples can be referred to PLA and PHBV due to post-crystallisation enthalpies and expectation of heat of fusion. A relation of 1/2.5 is expected for 50:50 blends (s.a.), which should lead to melting enthalpies for PLA of about 18 to 20 J g^{-1} or less if PLA has a lower crystallinity (Table 3, ΔH_m/3.5). For blends with molecular weights < 30 kDa, post-crystallisation enthalpies for transitions at ~ 103 ± 5 °C are in the same range. Blends with molecular weights > 30 kDa show higher post-crystallisation enthalpies, but exhibit two transitions at ~ 90 to 100 °C and ~ 110 °C, respectively. Therefore, we conclude that the quenched samples pass a post-crystallisation of PHBV or PLA from spinodally decomposed phases for blends with molecular weights < 30 kDa. Blends with molecular weights > 30 kDa pass this post-crystallisation from phase separated frozen melts. Due to higher mobility and miscibility of low molecular weight blends, leading to interaction of PLA and PHB in the spinodally-decomposed phases, less perfect crystals will be formed leading to a lower melting temperature and changes in peak contour.

The thermograms of the second heating scan after controlled cooling (Figure 7c-d) show no T_{cc} of a PHBV phase, but a T_{cc} belonging to a disturbed PLA phase between 95–105 °C. In most samples, only one clear T_g belonging to PLA can be detected (*k*-values indicating immiscibility, Figure 5). Therefore, it can be concluded that, during cooling, the spinodally-decomposed phases (s.a.) show crystallisation of PHBV from the PHBV-rich phase and PLA-rich phase (Table 3, ΔH_c of about 40 J g^{-1} indicates an overall crystallinity of PHBV of about 60 %) and post-crystallisation of PLA from the PLA-rich phase. The samples with molecular weights greater than 30 kDa exhibit a melting transition higher than 170 °C, and the highest post-crystallisation temperatures. The high melting transition can be interpreted as a pure undisturbed PHBV phase (T_m ~ 172 °C, own measurement of high M_n PHBV) in contrast to melting transition of the quenched samples. Due to the very high temperature, the post-crystallisation should result from PLA-rich phases, but due to two peaks below 170 °C also some PHBV crystallisation should take place.

The post-crystallization temperatures of the blends with PLA having 15 kDa molecular weight (15/15 and 15/28 PLA/PHBV blends) in the quenched samples and in the control-cooled samples, disturb the trend of temperatures in the blends with molecular weights below 30 kDa. This behaviour may be due to the broadness of molecular weight distribution (2.2, see materials and methods). Due to GPC measurements, this PLA sample includes small amounts of high molecular weight PLA with M_n in the range of 100 kDa. Therefore, spinodal decomposition or phase separation due to immiscibility in the melt will be altered to some extent, leading to phases depleted on PLA. These phases may trigger the post-crystallisation temperature.

Summary of the miscibility study

1) In 80:20 blends of PLA and PHBV, the miscibility in the melt at 190 °C and in the solid state (~100 °C) for molecular weights of the blend polymers below 30 kDa can be deduced from DSC measurements. The analysis of the *k*-value of the G-T-equation show higher free volume than expected by Fox equation.

2) 80:20 blends of low molecular weight PLA and PHBV (< 30 kDa) show crystallisation. The amorphous phase should be miscible due to T_g. The analysis of T_g with the G-T-equation indicates a high free volume.

3) No symmetrical behaviour in the 20:80 blends in relation to the 80:20 blends of PLA and PHBV is seen in the quenched samples. Post-crystallisation of a nearly pure PHBV phase occurs, but from T_g data, the miscibility in the amorphous phases of low molecular weight blends (about ~ 15 kDa of each polyester) can be deduced. A change in morphology is suggested from changes in post-crystallisation of PLA phases for blends with molecular weights > 30 kDa. Additional forces for separation of phases can be adopted.

4) Strong crystallisation of PHBV (due to enthalpy and absence of glass transition) takes place in the controlled cooling scan of the 20:80 blends. From T_g data, miscibility in the amorphous phases of low molecular weight blends (about ~ 15 kDa of each polyester) can be deduced.

5) In the 50:50 blends of PLA and PHBV, spinodal decomposition in the melt at 190 °C can be concluded from DSC measurements with post-crystallisation or crystallisation from these phases.

6) The T_g of the spinodal phases in the 50:50 blends of PLA and PHBV can be explained conclusively.

7) Analysing thermoanalytical data, a change in 'miscibility' for blends with molecular weights lower or higher than 30 kDa can be assumed. Concerning Flory-Huggins theory, a difference in solubility parameter of about 0.65 $J^{0.5}\,cm^{-1.5}$ can be evaluated.

8) The analysis of T_g with the G-T-equation gives insight into different behaviours of the amorphous phases.

Conclusion of the miscibility study

The evaluated difference in solubility parameter of 0.65 $J^{0.5}\,cm^{-1.5}$ does not differ in range from the mean of literature data for the determination of those parameters by incremental methods, and is higher than the data determined by Ohkoshi *et al.*[35] (high M_n PLA with low M_n amorphous atactic PHB), higher than the data of Koyama *et al* [30] (high M_n bacterial PHB with low M_n PLA (L-Isomer), and higher than the data of Ni *et al.* [34] (high M_n PLA with low M_n bacterial PHB (Table 2, 0.58, 0.54 and 0.57 $J^{0.5}\,cm^{-1.5}$, respectively). Interpretation of our results of PLA-rich blends (80:20) without consideration of the more PHBV-rich blends, would allow a parameter of about ~0.6 $J^{0.5}\,cm^{-1.5}$ for the blend with molecular weights of 37.5 and 39.5 kDa for PLA and PHBV, respectively. Analysis of T_g of the quenched sample shows slight miscibility in the melt. However, the analysis of the *k*-value of the G-T-equation indicates a change in quality of mixing, and the behaviour of the 50/50 blends cannot be explained with a solubility parameter difference of $\leq 0.6\ J^{0.5}\,cm^{-1.5}$. Part of the deviations may be due to variations in the molecular weight distribution and its influence on miscibility, as Flory-Huggins theory is valid for monodisperse systems. Another part may be due to interactions that depend on molecular weight and composition, as the analysis of the *k*-value of the G-T-equation indicates. The high value of about 2 (w_1 = PLA) for miscible blends, can be explained by less intense interactions between PLA and PHBV chains than between PHBV chains alone, leading to a higher free volume than expected in miscible blends. Those interactions are dominant if there is enough PLA in the blend and miscibility is thermodynamically allowed. In blends with high amounts of PHBV, sufficient contacts between PLA and PHBV are not possible, as the non-symmetrical course of the *k* values in the 80:20 and 20:80 blends of PLA and PHBV indicate. For miscibility, molecular weight must then be reduced for compensation which leads to higher mixing enthalpies. In general, good miscibility shall happen up to a certain content of PHBV, which depends on the enthalpic quality of the PHBV interchain interactions. Furukawa, Sato[23] report a modified morphology of 80:20 blends in comparison to 60:40, 40:60, and 20:80 blends of PLA and PHBV, respectively. Therefore, the combination of molecular weights of the components, which determines the entropic contribution of free mixing enthalpy and the PHBV interaction which, depending on composition, modulate the energy contribution of free miscibility enthalpy, are responsible for phase behaviour in the melt and for phase separation and nucleation during cooling. The nucleation will be responsible for the resulting crystallinity and morphology of the blend, and morphology will be important for all applied properties.

As the crystallization enthalpy of commercial types of PHBV are often high (here: ~ 90 J g^{-1} or 7.5–8 kJ mol^{-1}, pure PHBV; own measurement), outdoing free miscibility entropy, very high temperatures (or different molar volumes, see Figure 1a) are necessary to outperform crystallization by miscibility (from eq. 1 and $\Phi_1 = \Phi_2 = 0.5$, $V_{1m} = V_{2m}$, $V_m = 2V_{1m}$: $\Delta G = 11.4 \cdot T$ (J) for mixing one mole polymer with one mole polymer 2 (or $11.6 \cdot T$ (J) for PLA and PHBV with $V_{1m} = 0.8\ V_{2m}$, $V_m = 1.8\ V_{2m}$), even when free mixing enthalpy is zero and crystallization of PLA is negligible).

Real blends of PLA with PHBV for extrusion and injection moulding, therefore, should always be immiscible since molecular weights of components are too high for miscibility. Nevertheless, molecular weight distribution can provide some fractions of lower molecular weight polymers that then can act as an interfacial compatibiliser, when the system can be quenched in the amorphous state during production. This may be the reason for the better dispersion of PHBV in PLA at weight fractions of 90/10,[27] preventing nucleation in the miscible phase.

The suppression of nucleation and crystallization of PHBV may be an optimisation strategy in PLA:PHBV blends, if other properties for the intended application are not disturbed too much.

This can be done by a) choosing the lowest PHBV concentration possible, b) using blend polymers with fractions of lower molecular weight polymers, c) using PHB-copolymers with lower crystallinities, or d) addition of additives, which decreases mobility and nucleation of PHBV e.g., compatible high T_g polymers.

Part II

Study on mechanical and barrier properties of PLA:PHBV blends with selected additives

For a further analysis, different additives were selected to improve the miscibility of PLA:PHBV blends and analyse their influence on mechanical

and barrier properties of the blends. The following work aims at the understanding of the interaction and stability of the two phases in a blend system, and at the influence of boundary active components on the barrier properties. In immiscible blends, the interface between the matrix polymer and the dispersed phase is an influencing factor for many properties.[48] To enhance the interface between PLA and PHBV, compatibilisers are often used to alter the interfacial tension. In a ternary system, the compatibiliser compatibilises the dispersed phase when the spreading coefficient is positive.[48,66,67]

From literature data, surface tension of the highly polar polyesters PLA and PHBV of about 40–43 mJ m^{-2} for PLA[68,69] 47–49 mJ m^{-2} for PHB/PHBV[69,70] can be derived. The compatibiliser should therefore have a surface tension in this range. This can be done by using random copolymers[71] and block-copolymers of the components.[48] Another possible approach is the application of the solubility parameter concept, finding components with similar parameters as listed in Table 1. Segmented and up to random copolymers can be produced by tranesterification. Block-copolymers can be produced by reactive extrusion of the polymers with peroxides, as done for PLA/PBAT, PLA/PBS and PLA/PCL blends.[72–74] To alter the live-time of generated radicals and therefore alter the possibility of diffusion, so-called 'vector-fluids' were used.[66] Additionally, 'surfactants' based on ambipolar molecules with a miscible polar component were used.

The following substances were chosen and blended as described in the section 'Methods'. The substances are listed according to the different approaches:

Surface-active compatibilisers

– PEG-PE 1400: Poly-(ethylene-block-polyethylene glycol) (50 % PEG, M_n: 1400 Da); obtained from Sigma-Aldrich Chemie GmbH, Taufkirchen, Germany;

– PEGDO: Polyethylene glycol 400 dioleat (M_n = 914 Da), obtained from Sigma-Aldrich Chemie GmbH, Taufkirchen, Germany;

– PMMA: Polymethyl methacrylate PLEXIGLAS® 7N Degussa-Röhm Formmassen; obtained from Evonik Industries AG, Essen, Germany;

Peroxides

– DCP: Dicumyl peroxide Perkadox BC-FF, 99 %; obtained from Akzo Nobel Packaging Coatings GmbH, Hilden, Germany;

– VB: Divinyl benzene, 80 %, technical grade; obtained from Sigma-Aldrich Chemie GmbH, Taufkirchen, Germany;

– HAD: Hexan diol diacrylate, 90 %, technical grade; obtained from Sigma-Aldrich Chemie GmbH, Taufkirchen, Germany;

– DEGDM: Diethylene glycol dimethacyrlate, 95 %, obtained from Sigma-Aldrich Chemie GmbH, Taufkirchen, Germany;

– PEGDO: s.a;

Transesterification catalysts

(all obtained from Sigma-Aldrich Chemie GmbH, Taufkirchen, Germany):

– $Fe(acac)_3$: Iron(III) acetyl acetonate
– $Zr(acac)_4$: Zirconium(IV) acetyl acetonate
– $Zn(acac)_2$: Zinc(II) acetyl acetonate
– $Cu(acac)_2$: Copper(II) acetyl acetonate
– TiBu: Titanium butylate
– Zn acetate: Zinc(II) acetate mono hydrate

Different molecular weights

For modulating the molecular weight and crystallisation morphology of PHBV, PHBV was partially crosslinked by the addition of 0.1 % DCP in a separate compounding step. Molecular weights were affected only to a slight extent, essentially the molecular weight distribution was altered to some extent (M_n: 122 kDa, M_w: 343 kDa). The modified PHBV was then processed with PLA and 0.5 % transesterificate.

All blends were processed in a PLA:PHBV ratio of 75:25 because of a better miscibility behaviour in PLA-rich blends, as discussed in part I and due to cost performance. The blends were processed in a cast film extrusion line, and subsequently characterised regarding their mechanical and barrier properties:

Mechanical properties

The mechanical properties of the prepared samples are listed in Table 4. The results reveal the high strength of pure PLA with a YM of 3169 N mm^{-2}, σ of 72 N mm^{-2}, and a ε of 3.6 %, which is in accordance with other literature.[45,75] In contrast, PHBV shows lower strength (σ 28 N mm^{-2}) and elongation at break (ε 1.2 %). The brittle behaviour and low mechanical flexibility of PHBV has already been reported in literature.[76] The reference blend without additives has a higher YM than the base biopolymers. The σ is more than double compared to pure PHBV. Especially, the ε is significantly increased, which proves the concept of increasing the flexibility by a blend system.

The blends additivated by compatibilisers show YM close to the value of pure PHBV but much higher σ compared to pure PHBV. Interestingly, the ε increased to 11 – 27 % but only in machine direc-

tion (MD). The strongest influence was observed with PMMA used as surface-active compatibiliser. This may be due to its high T_g (~110 °C) which altered the mobility of PLA and PHBV, and thus the blends' morphology.

The samples with the peroxides show varying trends. Using the peroxide (DCP) without the 'vector fluid', YM and σ are not changed significantly. By using the combined system, a loss in σ can be seen, which is more pronounced at higher peroxide concentrations. YM and ε are affected significantly only by the combined system DCP + VB. The most suitable combined additive system turns out to be DCP + VB. For these blends with DCP + VB, we can conclude that, with an increasing amount of both additives, the YM and σ decrease while the ε increases, which supports the proof of an effective increase in the miscibility of the base materials.

For the samples with the transesterificate and modified PHBV, a different setup of the tensile test had to be applied: the effective length between the clamps was reduced to 50 mm. This especially affected the values of YM, so YM should only be compared within this group. Analysing the samples with the transesterificates, YM is significantly decreased (due to the modified setup). The σ is in the same range as the samples with compatibilisers, and therefore slightly lower compared to the samples with peroxides. The ε is increased significantly with a maximum ε of 42 % for the 75:25 sample, which was added 2.5 % of transesterificated PLA:PHBV (50:50) using 0.37 % $Fe(acac)_3$ as catalyst (see section 'Methods'), followed by the samples with Zn-acetate. The samples with the modified PHBV as blend component for PLA reveal the lowest YM of all tested samples (again due to the modified setup), while the σ is comparable to the samples with compatibilisers. However, the ε turns out to be at a constant high level of 29 – 39 % throughout all catalysts.

Comparing with literature data, the increase of ε was stated to be 117 % (ε from 18 to 21 %) from pure PLA to a 90:10 PLA:PHBV blend by Guinault, Nguyen[77] or 111 % (ε from 5.6 to 6.2 %) from pure PLA to a 80:20 PLA:PHBV blend (by solvent casting) by Iannace, Ambrosio[45] which is significantly lower than for our sample with $Fe(acac)_3$ with 1188 % (ε from 3.55 to 42.19 %). This shows the effectiveness of the transesterifcation catalysts in a PLA:PHBV blend. But there are also data available showing mechanical properties in the same or higher range than our results: Gerard, Budtova[78] published an increase in ε of 1056 % (ε from 4.8 to 50.7 %) and Ma, Spoelstra[31] even report an increase of 5750 % (ε from 4 to 230 %) in both cases from pure PLA to a 80:20 PLA:PHBV blend. This unusually high increase may be due to the used PHBV with a content of 40 % of copolymer, leading to less crystallinity.

Barrier properties

Pure PLA reveals a significantly higher permeability compared to pure PHBV for all measured gases and water vapour (see Table 5). The factor of the permeabilities of PHBV to PLA is approx. four. Therefore, pure PHBV reveals high potential for applications with high barrier requirements. In literature, values for the OP of pure PLA are published at 198.7 cm^3 (STP) 100 µm m^{-2} d^{-1} bar^{-1} (corresponds to 2.3 $\cdot 10^{-18}$ m^3 m m^{-2} s^{-1} Pa^{-1})[75] (processed by thermo-compressing) or at 167.6 cm^3 (STP) 100 µm m^{-2} d^{-1} bar^{-1} (corresponds to 1.94 $\cdot 10^{-18}$ m^3 m m^{-2} s^{-1} Pa^{-1})[72] for an extruded film, indicating the comparably low OP of the PLA material in our study (144.9 cm^3 (STP) 100 µm m^{-2} d^{-1} bar^{-1}). Also, the published values of WVTR of a pure PLA film (processed by solution-casting with a crystallisation time of 5 minutes) is at 52 (g 100 µm m^{-2} d^{-1})[9] significantly higher compared to our sample (26 g 100 µm m^{-2} d^{-1}). The low WVTR of pure PHBV is in accordance with literature data (5 g 100 µm m^{-2} d^{-1}, but for 50 % rh processed by extrusion coating).[8]

Due to the immiscibility of the pure materials (according to the Flory-Huggins-Theory), the surface between the two phases are expected to be less than optimal. Therefore, the barrier properties should be lower (higher diffusion coefficients) compared to their theoretical ones. Improvement of the interface should result in even lower permeabilities.

Since our results were lower than a calculated blend system (based on the additivity rule), for better comparison, we calculated the barrier properties of a layer structure. Based on the permeabilities of the pure base materials, a permeability of a fictive two-layer structure of PLA/PHBV was calculated to have a reference value for the blend systems. For calculating the permeability Q, and the permeation coefficient of the multilayer of a system with i layers, the following equation can be applied:[79,80]

$$Q = \frac{P}{l}; \tag{8}$$

$$\frac{1}{P_{multilayer}} = \frac{1}{l_{total}} \sum_{i=1}^{i=n} \frac{l_i}{P_i} \tag{9}$$

According to this layer theory, the permeabilities of a multilayer structure of PLA/PHBV 50/50 (equals a 50 µm/50 µm setup) and 75/25 (equals a 75 µm/25 µm setup) for water vapour and different gases, were calculated based on the results of the pure materials and are displayed in Table 6. The results of the fictive two-layer structures prove the influence of PHBV on decreasing the permeabilities.

Table 4 – *Mechanical properties of PLA:PHBV blends processed to cast films*

Ratio PLA: PHBV	Additive/ Peroxide/Catalyst (transester.)	Concentration [%] of the			Film thickness [μm]	Young's Modulus (YM) [N mm^{-2}]		Tensile strength (σ) [N mm^{-2}]		Elongation at break (ε) [%]	
		additive	peroxide	catalyst		MD	TD	MD	TD	MD	TD
100 : 0					46	3169 ± 175	3114 ± 106	71.6 ± 2.2	51.6 ± 1.8	3.55 ± 0.4	1.84 ± 0.0
0 : 100					42	2954 ± 156	2833 ± 229	28.0 ± 0.8	23.5 ± 2.7	1.15 ± 0.2	0.79 ± 0.1
75 : 25					51	3357 ± 28	3329 ± 81	64.1 ± 0.5	56.5 ± 0.7	14.46 ± 3.1	2.30 ± 0.2
75 : 25	PEG-PE 1400	2			55	2849 ± 221	2952 ± 115	50.8 ± 4.4	32.5 ± 1.6	19.26± 11.6	1.14 ± 0.0
75 : 25	PEGDO	2			49	3010 ± 159	2984 ± 70	52.4 ± 1.8	42.6 ± 2.3	10.71 ± 6.6	2.52 ± 0.8
75 : 25	PMMA	2			44	3044 ± 81	3125 ± 64	49.3 ± 3.4	44.2 ± 0.9	27.06 ± 9.0	1.56 ± 0.1
75 : 25	DCP		0.1		52	2954 ± 79	2938 ± 51	65.7 ± 1.4	48.1 ± 1.1	2.97 ± 0.1	8.19 ± 0.7
75 : 25	DCP		0.25		51	3286 ± 49	2856 ± 431	65.8 ± 1.1	41.3 ± 4.7	2.60 ± 0.1	–
75 : 25	DCP + VB	0.042	0.1		53	3304 ± 63	3410 ± 77	64.2 ± 1.0	48.3 ± 1.2	2.91 ± 0.6	2.45 ± 0.4
75 : 25	DCP + VB	0.15	0.25		47	2892 ± 174	2731 ± 269	52.4 ± 5.3	33.3 ± 5.1	6.61 ± 4.8	3.29 ± 2.2
75 : 25	DCP + VB	0.13	0.26		56	2478 ± 182	2611 ± 195	39.6 ± 3.9	32.2 ± 5.2	8.75 ± 6.6	3.83 ± 2.9
75 : 25	DCP + HDA	0.081	0.1		51	3216 ± 88	2954 ± 123	58.7 ± 1.8	41.6 ± 2.1	2.31 ± 0.1	5.73 ± 0.8
75 : 25	DCP + HDA	0.21	0.25		68	2894 ± 119	2326 ± 152	46.2 ± 3.6	22.9 ± 3.1	3.26 ± 1.3	1.35 ± 0.2
75 : 25	DCP + DEGDM	0.09	0.1		52	2960 ± 82	3073 ± 81	56.2 ± 1.9	40.0 ± 1.8	2.53 ± 0.1	1.95 ± 0.4
75 : 25	DCP + PEGDO	0.33	0.1		49	3001 ± 59	3056 ± 81	58.8 ± 1.1	44.6 ± 2.0	4.12 ± 1.8	2.56 ± 0.3
75 : 25	DCP + PEGDO	0.83	0.25		54	2736 ± 45	2639 ± 79	52.2 ± 2.0	34.6 ± 0.7	3.39 ± 1.4	2.76 ± 0.4
75 : 25	$Fe(acac)_3$	2.5		0.37	55	1573 ± 249	1623 ± 103	57.9 ± 3.9	48.7 ± 3.0	42.19± 19.8	7.53 ± 4.5
75 : 25	$Fe(acac)_3$	2.5		0.79	57	1520 ± 260	1181 ± 477	55.8 ± 2.8	46.4 ± 3.3	34.86± 14.9	8.11 ± 0.5
75 : 25	$Zr(acac)_4$	2.5		0.41	56	2476 ± 720	2541 ± 427	55.7 ± 8.2	50.0 ± 3.0	9.83 ± 5.45	3.76 ± 1.7
75 : 25	$Zr(acac)_4$	2.5		0.97	52	1994 ± 527	3386 ± 681	56.8 ± 4.8	44.5 ± 3.8	10.06 ± 3.4	2.26 ± 1.1
75 : 25	$Zn(acac)_2$	2.5		0.42	54	1139 ± 500	1164 ± 609	52.0 ± 2.3	43.2 ± 4.0	35.57± 18.5	6.38 ± 2.0
75 : 25	$Zn(acac)_2$	2.5		0.78	53	1869 ± 243	1845 ± 198	53.3 ± 2.4	42.8 ± 1.8	17.03 ± 6.4	4.00 ± 0.5
75 : 25	$Cu(acac)_2$	2.5		0.44	60	1275 ± 697	1053 ± 747	50.2 ± 4.1	38.9 ± 4.1	12.53 ± 4.6	4.03 ± 0.8
75 : 25	$Cu(acac)_2$	2.5		0.76	59	1683 ± 451	1197 ± 462	52.4 ± 3.8	34.2 ± 5.4	12.59 ± 2.6	3.38 ± 0.5
75 : 25	$TiBu_4$	2.5		0.94	52	1466 ± 540	1748 ± 332	50.7 ± 2.8	40.9 ± 1.8	28.74± 10.8	3.55 ± 0.5
75 : 25	Zn acetate	2.5		0.63	51	1286 ± 364	2002 ± 103	51.8 ± 2.4	41.3 ± 1.5	37.10± 16.6	4.09 ± 0.4
75 : 25	m. PBHV	0	0		55	1184 ± 689	1629 ± 311	51.9 ± 2.6	44.6 ± 2.5	36.38± 15.2	4.88 ± 1.6
75 : 25	m. PBHV Zr	2.5		0.91	55	1484 ± 552	1908 ± 232	49.4 ± 3.0	49.0 ± 2.3	26.42 ± 5.3	5.91 ± 2.2
75 : 25	m. PBHV Fe	2.5		0.79	57	1077 ± 606	1608 ± 418	50.7 ± 2.5	49.9 ± 2.1	29.01 ± 7.4	9.33 ± 3.7
75 : 25	m. PBHV Cu	2.5		0.76	55	1075 ± 360	1200 ± 481	50.6 ± 1.6	47.2 ± 1.8	39.13± 18.3	6.62 ± 2.4
75 : 25	m. PBHV Zn	2.5		0.78	55	827 ± 486	986 ± 281	49.4 ± 3.2	45.8 ± 1.7	29.67± 11.7	5.24 ± 0.6

A reference blend (PLA:PHBV 75:25) without additives shows low permeabilities for all gases and water vapour. However, this reference blend reveals to have lower permeabilities than the calculated values of a multilayer system with the same ratio of the biopolymers. The discussed interaction of PLA and PHBV by interpenetrating spherulites,[17] leading to interlamellar crystallisation of one phase into the other, may be the reason for this behaviour. Thereby, the mobility of gases in the amorphous phases of the blend is changed. Furthermore, the compatibilisation of (amorphous) interfaces by miscible low molecular weight fractions of the polymers, excluding high diffusion pathway of gases due to lack of adhesion, may increase the barrier properties.

Table 5 – *Barrier properties of PLA:PHBV blends processed to cast films*

Ratio PLA: PHBV	Additive/ Peroxide/Catalyst (transester.)	Concentration [%] of the			Film thickness [µm]	WVTR 23/85 [g 100 µm m^{-2} d^{-1}]	OP 23/50 [cm^3 100 µm m^{-2} d^{-1} bar^{-1}]	OP 23/0 [cm^3 100 µm m^{-2} d^{-1} bar^{-1}]	N_2-P 23/0 [cm^3 100 µm m^{-2} d^{-1} bar^{-1}]	CO_2-P 23/0 [cm^3 100 µm m^{-2} d^{-1} bar^{-1}]
		additive	peroxide	catalyst		Q	Q	Q	Q	Q
100 : 0					46	26.0 ± 1.0	144.9 ± 1.0	129.1 ± 4.1	19.2 ± 1.2	300 ± 18.4
0 : 100					42	6.3 ± 0.1	34.2 ± 1.3	30.2 ± 3.1	4.2 ± 0.4	101 ± 10.4
75 : 25					51	11.6 ± 0.4	57.9 ± 1.1	54.4 ± 4.0	7.7 ± 0.3	52 ± 3.1
75 : 25	PEG-PE 1400	2			55	12.2 ± 1.2	56.8 ± 2.8	52.0 ± 4.7	7.5 ± 0.3	113 ± 5.0
75 : 25	PEG-Oleat	2			49	11.3 ± 0.2	59.5 ± 3.0	52.6 ± 5.1	7.1 ± 0.6	110 ± 9.4
75 : 25	PMMA	2			44	11.9 ± 0.2	55.1 ± 0.1	46.7 ± 4.0	6.2 ± 0.2	104 ± 6.0
75 : 25	DCP		0.1		52	13.9 ± 0.5	68.6 ± 7.4	47.0 ± 0.3	8.2 ± 0.1	132 ± 10.0
75 : 25	DCP		0.25		51	14.0 ± 1.1	78.1 ± 2.9	73.6 ± 3.4	9.9 ± 0.8	164 ± 6.3
75 : 25	DCP + VB	0.042	0.1		53	17.7 ± 0.8	72.6 ± 0.0	61.5 ± 4.8	8.2 ± 0.8	133 ± 9.6
75 : 25	DCP + VB	0.15	0.25		47	17.6 ± 1.0	113.1 ± 5.0	73.0 ± 13.5	9.6 ± 2.0	162 ± 40.4
75 : 25	DCP + VB	0.13	0.26		56	19.3 ± 1.3	72.3 –	108.0 ± 76.5	25.2 ± 24.2	216 ± 217
75 : 25	DCP + HDA	0.081	0.1		51	13.8 ± 0.8	70.7 –	89.8 ± 40.5	34.0 ± 37.5	147 ± 24.1
75 : 25	DCP + HDA	0.21	0.25		68	21.1 ± 1.6	107.7 ± 10.1	104.5 ± 7.2	19.3 ± 2.0	122 ± 5.9
75 : 25	DCP + DEGDM	0.09	0.1		52	14.0 ± 0.2	69.9 ± 1.5	56.3 ± 27.8	4.2 ± 0.7	101 ± 34.3
75 : 25	DCP + PEGDO	0.33	0.1		49	13.4 ± 0.1	72.8 ± 4.8	26.3 ± 9.8	4.3 ± 0.3	72 ± 4.4
75 : 25	DCP + PEGDO	0.83	0.25		54	17.4 ± 0.8	94.5 ± 0.0	45.5 ± 3.7	6.1 ± 0.4	105 ± 6.6
75 : 25	$Fe(acac)_3$	2.5		0.37	54.6	12.6 ± 0.4	65.2 ± 5.8	48.3 ± 1.0	6.6 ± 0.4	209 ± 0.0
75 : 25	$Fe(acac)_3$	2.5		0.79	56.9	12.4 ± 0.5	63.5 ± 6.0	57.3 ± 1.8	7.3 ± 0.6	178 ± 5.2
75 : 25	$Zr(acac)_4$	2.5		0.41	55.9	12.0 ± 0.3	63.3 ± 4.2	50.0 ± 0.4	6.7 ± 0.2	273 ± 5.1
75 : 25	$Zr(acac)_4$	2.5		0.97	52.2	12.6 ± 0.7	69.1 ± 8.5	51.4 ± 0.7	6.8 ± 0.2	274 ± 0.0
75 : 25	$Zn(acac)_2$	2.5		0.42	53.8	11.7 ± 0.2	58.4 ± 4.9	48.2 ± 4.3	6.8 ± 0.5	223 ± 5.2
75 : 25	$Zn(acac)_2$	2.5		0.78	53.5	11.6 ± 0.4	55.3 ± 5.0	46.5 ± 0.6	6.7 ± 0.5	209 ± 0.0
75 : 25	$Cu(acac)_2$	2.5		0.44	59.7	11.9 ± 0.2	57.9 ± 1.9	49.9 ± 2.4	6.9 ± 0.3	344 ± 1.4
75 : 25	$Cu(acac)_2$	2.5		0.76	58.6	12.4 ± 0.3	63.9 ± 0.0	52.6 ± 1.1	7.1 ± 1.4	277 ± 7.8
75 : 25	$TiBu_4$	2.5		0.94	51.9	10.1 ± 0.2	59.2 ± 4.4	51.2 ± 0.9	6.2 ± 0.7	215 ± 13.8
75 : 25	Zn acetate	2.5		0.63	50.9	9.3 ± 0.5	69.5 ± 14.0	45.2 ± 1.7	5.9 ± 0.1	222 ± 0.7
75 : 25	m. PBHV				54.6	11.5 ± 0.5	58.6 ± 4.1	49.6 ± 4.1	6.6 ± 0.5	183 ± 5.6
75 : 25	m. PBHV Zr	2.5		0.91	54.8	11.9 ± 0.3	56.2 ± 1.9	45.7 ± 2.2	5.8 ± 0.6	193 ± 4.4
75 : 25	m. PBHV Fe	2.5		0.79	57.3	11.8 ± 0.1	57.8 ± 4.0	50.2 ± 4.0	6.6 ± 0.4	258 ± 13.5
75 : 25	m. PBHV Cu	2.5		0.76	54.6	12.0 ± 0.2	56.5 ± 1.2	47.7 ± 5.5	6.2 ± 0.7	187 ± 9.0
75 : 25	m. PBHV Zn	2.5		0.78	55.0	12.0 ± 0.3	56.7 ± 3.0	46.3 ± 4.9	6.4 ± 0.3	292 ± 16.1

Table 6 – *Calculated permeabilities for a two-layer-structure*

Multilayer PLA/PHBV	WVTR 23/85 [g 100 µm m^{-2} d^{-1}]	OP 23/50 [cm^3 100 µm m^{-2} d^{-1} bar^{-1}]	OP 23/0 [cm^3 100 µm m^{-2} d^{-1} bar^{-1}]	N_2-P 23/0 [cm^3 100 µm m^{-2} d^{-1} bar^{-1}]	CO_2-P 23/0 [cm^3 100 µm m^{-2} d^{-1} bar^{-1}]
50 / 50	10.1	55.3	49.0	7.0	151
75 / 25	14.6	79.8	70.7	9.8	201

The permeabilities of the samples with different compatibilisers are found to be comparable to the reference blend for all applied compatibilisers, and are significantly lower than the calculated values of a 75/25 multilayer setup.

The permeabilities of the samples with peroxides are higher than those of the samples with compatibilisers. The values for the WVTR range from 13.4 to 21.1 g 100 μm m^{-2} d^{-1} and are higher than the calculated values of a multilayer system. The OP at humid conditions (50 % rh) are higher than the values of the samples with compatibilisers, and differ depending on the additive. The lowest permeabilities throughout all permeation measurements show the additives DCP + DEGDM and DCP + PEGDO. Especially their low N_2-P and CO_2-P is of interest. In general, the values with peroxide compatibilisation show a higher distribution than the other samples, especially at higher amounts of peroxides. This may be due to the possibility of small amounts of insoluble gel-particles, offering high diffusion pathways.

The samples compatibilised with transesterificates of PLA and PHBV by several catalysts reveal the lowest permeabilities of all approaches for a stable blend system. The variation between the samples with different transesterification catalysts is low, which favours the effectiveness of this approach. All samples show significantly lower values compared to the other samples (with compatibilisers and peroxides), and compared to the calculated permeabilities. The lowest permeability is reached by the sample with Zn-acetate as transesterification catalyst.

The samples with peroxide-modified PHBV show permeabilities in the range of the samples with the transesterification catalysts. All samples of this group show WVTR lower than 12 g 100 μm m^{-2} d^{-1}, while their OP has maximum values of 50 (for 0 % rh) and 59 cm^3 100 μm m^{-2} d^{-1} bar^{-1} (for 50 % rh). This high reproducibility of the barrier properties throughout all applied transesterificates in the modified PHBV leads to the conclusion that the morphology is not changed significantly by the transesterificates.

By summarising these results, we can state that the addition of peroxides does not decrease the barrier properties in a way that can be achieved by compatibilisers, transesterification catalysts and modified molecular weights. This effect is in accordance with the effect on the mechanical properties as discussed before.

In summary, our results suggest that blending PLA with 25 % PHBV by different methods leads to a reduction in the YM and σ, while the ε is increased. In addition, the effect on the barrier properties is significant: The WVTR as well as OP, N_2-P and CO_2-P were decreased compared to pure PLA. The calculated values of a 75/25 multilayer structure are significantly higher than our samples for all measured permeabilities, except the samples with peroxides. In fact, the measured permeabilities of our blends are even in the range of a 50/50 two-layer system (see Table 6). The OP of the blends show much lower values compared to data from literature for a 90:10 PLA:PHBV blend (157.2 cm^3 (STP) 100 μm m^{-2} d^{-1} bar^{-1}).[77] But there is also data available which report lower OP of a 75:25 PLA:PHBV blend (2.2 cm^3 μm m^{-2} d^{-1} atm^{-1}).[13] There are different opinions of how strongly crystallinity is affecting the OP of PLA films.[72,81] Courgneau, Domenek[75] published that a blend with 17 % wt. ATBC in order to improve PLAs' mechanical properties showed a OP of 432.9 cm^3 (STP) 100 μm m^{-2} d^{-1} bar^{-1} (corresponds to $5.01 \cdot 10^{-18}$ m^3 m m^{-2} s^{-1} Pa^{-1}).[75] Also, the authors Courgneau, Domenek[10] reported an increasing OP by adding different low-molecular compatibilisers in PLA.[10] Contrary to these results, the samples analysed in our study behaved differently and decreased the OP significantly. The effectiveness of the compatibilisation of our blends can be concluded by the comparison with Zembouai, Kaci[13]: The authors report a WVTR for PLA of 26.9 g 100 μm m^{-2} d^{-1} (corresponds to 2.24 g m^{-1} s^{-1} Pa^{-1} 10^{-11}) and for a 75:25 PLA:PHBV blend of 20.7 g 100 μm m^{-2} d^{-1} (corresponds to 1.73 g m^{-1} s^{-1} Pa^{-1} 10^{-11}), while we could decrease the WVTR from 26.0 g 100 μm m^{-2} d^{-1} to 9.3 g 100 μm m^{-2} d^{-1}. As discussed before for PLA, also by the addition of ATBC in PHBV, an increase in WVTR can be stated.[8] Therefore, the approach presented in this work is a suitable way to improve the mechanical properties and simultaneously decrease the permeabilities.

However, these results suggest that there is a humidity-dependant permeability of the blends. The average OP at 0 % rh is 70 % to 90 % of the OP at 50 % rh. Additionally, the permselectivity of these blend systems can be analysed accordingly: the ratio between the N_2-P and OP is approx. at 1:6.7 to 1:8.3, while the ratio between OP and CO_2-P is approx. 1:5 if the break through time is considered. However, these results of permselectivity are not in accordance with literature.[81]

Conclusion

Concluding from the presented results, there is a suitable concentration of PHBV of about 20–35 % in PLA that shows the most improved properties (which is supported by Ma, Spoelstra[31]). Above this concentration, the formation of co-continuous phases or spinodal decomposition is favoured, even for lower molecular weight fractions of the polymers, and the inherent brittleness of PLA and PHBV is not decreased sufficiently. Furthermore, the interaction between PLA and PHBV in the interlamellar

areas of the spherulites are better in a 75:25 than in a 50:50 blend.[17] Blends already with this low concentration of PHBV form well compatible systems without a long-term demixing process, which will happen in metastabile 50:50 blends. In addition, the effectiveness with these small amounts of PHBV in terms of decreasing the barrier properties supports this conclusion. Our samples with only 25 % PHBV decreased the WVTR to 46 % and the OP to 40 % of the respective permeability of pure PLA.

The influence of the different approaches for changing interfacial properties by compatibilisers should be investigated in more detail for the evaluation of the functionality and reproducibility of such systems.

ACKNOWLEDGEMENT

The authors wish to acknowledge the financial support from the research association, 'Industrievereinigung für Lebensmitteltechnologie und Verpackung e.V.' by the ‚AiF' under the program of industrial research of the 'Industrielle Gemeinschaftsforschung (IGF)' of the 'Bundesministerium für Wirtschaft und Energie' under the grant agreement 'IGF-Vorhaben 16115 N'.

References

1. *Endres, H.-J., Siebert-Raths, A.,* Engineering biopolymers: Markets, manufacturing, properties and applications., Hanser Verlag, München, 2011. doi: http://dx.doi.org/10.3139/9783446430020
2. *Gupta, A. P., Kumar, V.,* New emerging trends in synthetic biodegradable polymers – Polylactide: A critique, Eur. Polym. J. **43**(10) (2007) 4053. doi: http://dx.doi.org/10.1016/j.eurpolymj.2007.06.045
3. *Albuquerque, M. G. E., Martino, V., Pollet, E., Avérous, L., Reis, M. A. M.*, Mixed culture polyhydroxyalkanoate (PHA) production from volatile fatty acid (VFA)-rich streams: Effect of substrate composition and feeding regime on PHA productivity, composition and properties, J. Biotechnol. **151**(1) (2011) 66. doi: http://dx.doi.org/10.1016/j.jbiotec.2010.10.070
4. *Rhu, D. H., Lee, W. H., Kim, J. Y., Choi, E. R.*, Polyhydroxyalkanoate (PHA) production from waste, Water Sci. Technol. **48**(8) (2003) 221.
5. *Chanprateep, S.,* Current trends in biodegradable polyhydroxyalkanoates. J. Biosci. Bioeng. **110**(6) (2010) 621. doi: http://dx.doi.org/10.1016/j.jbiosc.2010.07.014
6. *Poirier, Y., Nawrath, C., Somerville, C.,* Production of Polyhydroxyalkanoates, a Family of Biodegradable Plastics and Elastomers, in Bacteria ansd Plants, Nat Biotechnol. **13**(2) (1995) 142. doi: http://dx.doi.org/10.1038/nbt0295-142
7. *Doyle, C., Tanner, E. T., Bonfield, W.,* In vitro and in vivo evaluation of polyhydroxybutyrate and of polyhydroxybutyrate reinforced with hydroxyapatite, Biomaterials **12**(9) (1991) 841. doi: http://dx.doi.org/10.1016/0142-9612(91)90072-I
8. *Kuusipalo, J.*, PHB/V in Extrusion Coating of Paper and Paperboard—Study of Functional Properties. Part II, J. Polym. Environ., **8**(2) (2000) 49. doi: http://dx.doi.org/10.1023/A:1011565519440
9. *Tsuji, H., Okino, R., Daimon, H., Fujieet, K.*, Water vapor permeability of poly(lactide)s: Effects of molecular characteristics and crystallinity, J. Appl. Polym. Sci. **99**(5) (2006) 2245. doi: http://dx.doi.org/10.1002/app.22698
10. *Courgneau, C. Domenek, S., Guinault, A., Avérous, L., Ducruet, V.*, Analysis of the Structure-Properties Relationships of Different Multiphase Systems Based on Plasticized Poly(Lactic Acid), J. Polym. Environ. **19**(2) (2011) 362. doi: http://dx.doi.org/10.1007/s10924-011-0285-5
11. *Tsuji, H. Tsuruno, T.,* Water Vapor Permeability of Poly(L-lactide)/Poly(D-lactide) Stereocomplexes, Macromol. Mater. Eng. **295**(8) (2010) 709. doi: http://dx.doi.org/10.1002/mame.201000071.
12. *Fabra, M. J., Lopez-Rubio, A., Lagaron, J. M.*, High barrier polyhydroxyalcanoate food packaging film by means of nanostructured electrospun interlayers of zein, Food Hydrocolloids **32**(1) (2013) 106. doi: http://dx.doi.org/10.1016/j.foodhyd.2012.12.007
13. *Zembouai, I., Kaci, M., Bruzaud, S., Benhamida, A., Corre, Y. M., Grohens, Y.*, A study of morphological, thermal, rheological and barrier properties of Poly(3-hydroxybutyrate-Co-3-Hydroxyvalerate)/polylactide blends prepared by melt mixing,. Polym. Test. **32**(5) (2013) 842. doi: http://dx.doi.org/10.1016/j.polymertesting.2013.04.004
14. *Boufarguine, M., Guinault, A., Miquelard-Garnier, G., Sollogoub., C.*, PLA/PHBV Films with Improved Mechanical and Gas Barrier Properties, Macromol. Mater. Eng. **298**(10) (2013) 1065. doi: http://dx.doi.org/10.1002/mame.201200285
15. *Abdelwahab, M. A., Flynn, A., Chiou, B. S., Imam, S., Orts, W., Chiellini, E.*, Thermal, mechanical and morphological characterization of plasticized PLA–PHB blends, Polym. Degrad. Stab. **97**(9) (2012) 1822. doi: http://dx.doi.org/10.1016/j.polymdegradstab.2012.05.036
16. *Bartczak, Z., Galeski, A., Kowalczuk, M., Sobota, M., Malinowski, R.*, Tough blends of poly(lactide) and amorphous poly([R,S]-3-hydroxy butyrate) – morphology and properties, Eur. Polym. J. **49**(11) (2013) 3630. doi: http://dx.doi.org/10.1016/j.eurpolymj.2013.07.033
17. *Blümm, E. Owen, A. J.,* Miscibility, crystallization and melting of poly(3-hydroxybutyrate)/ poly(l-lactide) blends. Polymer **36**(21) (1995) 4077. doi: http://dx.doi.org/10.1016/0032-3861(95)90987-d.
18. *Chang, L. Woo, E. M.*, Effects of molten poly(3-hydroxybutyrate) on crystalline morphology in stereocomplex of poly(L-lactic acid) with poly(D-lactic acid*)*. Polymer **52**(1) (2011) 68. doi: http://dx.doi.org/10.1016/j.polymer.2010.11.028
19. *Domb, A. J.*, Degradable polymer blends. I. Screening of miscible polymers. J. Polym. Sci. Polym. Chem.. **31**(8) (1993) 1973. doi: http://dx.doi.org/10.1002/pola.1993.080310805
20. *El-Hadi, A. M.,* Effect of processing conditions on the development of morphological features of banded or non-banded spherulites of poly(3-hydroxybutyrate) (PHB) and polylactic acid (PLLA) blends Polym. Eng. Sci. **51**(11) (2011) 2191. doi: http://dx.doi.org/10.1002/pen.21991
21. *Ferreira, B. M. P., Zavaglia, C. A. C., Duek, E. A. R.,* Films of PLLA/PHBV: thermal, morphological, and mechanical characterization. J. Appl. Polym. Sci. **86**(11) (2002) 2898. doi: http://dx.doi.org//10.1002/app.11334

22. *Focarete, M. L., Scandola, M., Dobrzynski, P., Kowalczuk, M.*, Miscibility and Mechanical Properties of Blends of (L)-Lactide Copolymers with Atactic Poly(3-hydroxybutyrate), Macromolecules **35**(22) (2002) 8472. doi: http://dx.doi.org/10.1021/ma020940z
23. *Furukawa, T., Sato, H., Murakami, R., Zhang, J., Duan, Y. X., Noda, I., Ochiai, S., Ozaki, Y.*, Structure, Dispersibility, and Crystallinity of Poly(hydroxybutyrate)/Poly(l-lactic acid) Blends Studied by FT-IR Microspectroscopy and Differential Scanning Calorimetry, Macromolecules **38**(15) (2005) 6445. doi: http://dx.doi.org/10.1021/ma0504668
24. *Furukawa, T., Sato, H., Murakami, R., Zhang, J., Noda, I., Ochiai, S., Ozaki, Y.*, Comparison of miscibility and structure of poly(3-hydroxybutyrate-co-3-hydroxyhexanoate)/poly(l-lactic acid) blends with those of poly(3-hydroxybutyrate)/poly(l-lactic acid) blends studied by wide angle X-ray diffraction, differential scanning calorimetry, and FTIR microspectroscopy, Polymer **48**(6) (2007) 1749. doi: http://dx.doi.org/10.1016/j.polymer.2007.01.020
25. *Gao, Y., Kong, L., Zhang, L., Gong, Y., Chen, G., Zhao, N., Zhang, X.,* Improvement of mechanical properties of poly(dl-lactide) films by blending of poly(3-hydroxybutyrate-co-3-hydroxyhexanoate), Eur. Polym. J. **42**(4) (2006) 764. doi: http://dx.doi.org/10.1016/j.eurpolymj.2005.09.028
26. *Kikkawa, Y., Suzuki, T., Kanesato, M., Doi, Y., Abe, H.*, Morphology and molten-state rheology of polylactide and polyhydroxyalkanoate blends, Biomacromolecules **10**(4) (2009) 1013. doi: http://dx.doi.org/10.1021/bm900117j
27. *Gerard, T., Budtova, T,,* Morphology and molten-state rheology of polylactide and polyhydroxyalkanoate blends. Eur. Polym. J. **48**(6) (2012) 1110. doi: http://dx.doi.org/10.1016/j.eurpolymj.2012.03.015
28. *Focarete, M. L., Ceccorulli, G., Scandola, M., Kowalczuk, M.,* Further Evidence of Crystallinity-Induced Biodegradation of Synthetic Atactic Poly(3-hydroxybutyrate) by PHB-Depolymerase A from Pseudomonas lemoignei. Blends of Atactic Poly(3-hydroxybutyrate) with Crystalline Polyesters, Macromolecules **31**(24) (1998) 8485. doi: http://dx.doi.org/10.1021/ma981115e
29. *Koyama, N., Doi, Y.*, Miscibility, Thermal Properties, and Enzymatic Degradability of Binary Blends of Poly[(R)-3-hydroxybutyric acid] with Poly(ε-caprolactone-co-lactide). Macromolecules, **29**(18) (1996) 5843. doi: http://dx.doi.org/10.1021/ma960119l
30. *Koyama, N. Doi, Y.*, Miscibility of binary blends of poly[(R)-3-hydroxybutyric acid] and poly[(S)-lactic acid], Polymer **38**(7) (1997) 1589. doi: http://dx.doi.org/10.1016/S0032-3861(96)00685-4
31. *Ma, P., Spoelstra, A. B., Schmit, P., Lemstra, P. J.*,-co-β-hydroxyvalerate) with high β-hydroxyvalerate content, Eur. Polym. J. **49**(6) (2013) 1523. doi: http://dx.doi.org/10.1016/j.eurpolymj.2013.01.016
32. *Modi, S., Koelling, K., Vodovotz, Y.*, Miscibility of poly(3-hydroxybutyrate-co-3-hydroxyvalerate) with high molecular weight poly(lactic acid) blends determined by thermal analysis, J. Appl. Polym. Sci. **124**(4) (2012) 3074. doi: http://dx.doi.org/10.1002/app.35343
33. *Nanda, M. R., Misra, M., Mohanty, A. K.*, The Effects of Process Engineering on the Performance of PLA and PHBV Blends, Macromol. Mater. Eng. **296**(8) (2011) 719. doi: http://dx.doi.org//10.1002/mame.201000417
34. *Ni, C., Luo, R., Xu, K., Chen, G. Q.*, Thermal and crystallinity property studies of poly (L-lactic acid) blended with oligomers of 3-hydroxybutyrate or dendrimers of hydroxyalkanoic acids, J. Appl. Polym. Sci. **111**(4) (2009) 1720. doi: http://dx.doi.org/10.1002/app.29182
35. *Ohkoshi, I., Abe, H., Doi, Y.*, Miscibility and solid-state structures for blends of poly[(S)-lactide] with atactic poly[(R,S)-3-hydroxybutyrate], Polymer **41**(15) (2000) 5985. doi: http://dx.doi.org/10.1016/S0032-3861(99)00781-8
36. *Park, J. W., Doi, Y., Iwata, T.*, Uniaxial Drawing and Mechanical Properties of Poly[(R)-3-hydroxybutyrate]/Poly(l-lactic acid) Blends, Biomacromolecules **5**(4) (2004) 1557. doi: http://dx.doi.org/10.1021/bm049905l
37. *Reeve, M. S., McCarthy, S. P., Gross, R. A.*, Preparation and characterization of (R)-poly(.beta.-hydroxybutyrate)-poly(.epsilon.-caprolactone) and (R)-poly(.beta.-hydroxybutyrate)-poly(lactide) degradable diblock copolymers, Macromolecules **26**(5) (1993) 888. doi: http://dx.doi.org/10.1021/ma00057a002
38. *Takagi, Y., Yasuda, R., Yamaoka, M., Yamane, T.*, Morphologies and mechanical properties of polylactide blends with medium chain length poly(3-hydroxyalkanoate) and chemically modified poly(3-hydroxyalkanoate), J. Appl. Polym. Sci. **93**(5) (2004) 2363. doi: http://dx.doi.org/10.1002/app.20734
39. *Wasantha, K., Gunaratne, L. M., Shanks, R. A.*, Miscibility, melting, and crystallization behavior of poly(hydroxybutyrate) and poly(D,L-lactic acid) blends, Polym. Engin. Sci. **48**(9) (2008) 1683. doi: http://dx.doi.org/10.1002/pen.21051
40. *Yoon, J.-S., Lee, W.-S., Kim, K.-S.; Chin, I.-J., Kim, M.-N., Kim, C.,* Effect of poly(ethylene glycol)-block-poly(L-lactide) on the poly[(R)-3-hydroxybutyrate]/poly(L-lactide) blends, Eur. Polym. J. **36**(2) (2000) 435. doi: http://dx.doi.org/10.1016/S0014-3057(99)00068-3
41. *Zhang, L., Xiong, C., Deng, X.*, Biodegradable polyester blends for biomedical application, J. Appl. Polym. Sci. **56** (1995) 103. doi: http://dx.doi.org/10.1002/app.1995.070560114
42. *Zhang, L., Xiong, C., Deng, X.,* Miscibility, crystallization and morphology of poly(β-hydroxybutyrate)/poly(d,l-lactide) blends, Polymer **37**(2) (1996) 235. doi: http://dx.doi.org/10.1016/0032-3861(96)81093-7
43. *Zhang, J., Sato, H., Furukawa, T., Tsuji, H., Noda, I., Ozaki, Y.,* Crystallization Behaviors of Poly(3-hydroxybutyrate) and Poly(l-lactic acid) in Their Immiscible and Miscible Blends, J. Phys. Chem. B **110**(48) (2006) 24463. doi: http://dx.doi.org/10.1021/jp065233c
44. *Zhao, H., Cui, Z., Wang, X., Turng, L.-S., Peng, X.*, Processing and characterization of solid and microcellular poly(lactic acid)/polyhydroxybutyrate-valerate (PLA/PHBV) blends and PLA/PHBV/Clay nanocomposites, Compos. Part B-Eng. **51** (2013) 79. doi: http://dx.doi.org/10.1016/j.compositesb.2013.02.034
45. *Iannace, S., Ambrosio, L., Huang, S. J., Nicolais, L.*, Poly(3-hydroxybutyrate)-co-(3-hydroxyvalerate)/Poly-L-lactide blends: Thermal and mechanical properties, J. Appl. Polym. Sci. **54**(10) (1994) 1525. doi: http://dx.doi.org/10.1002/app.1994.07054101
46. *Wu, L., Chen, S., Li, Z., Xu, K., Chen, G.-Q.*, Synthesis, characterization and biocompatibility of novel biodegradable poly[((R)-3-hydroxybutyrate)-block-(D,L-lactide)-block-(ε-caprolactone)] triblock copolymers, Polym. Int. **57** (2008) 939. doi: http://dx.doi.org/10.1002/pi.2431
47. *Flory, P. J.,* Thermodynamics of High Polymer Solutions. J. Chem. Phys., **10**(1) (1942) 51. doi: http://dx.doi.org/10.1063/1.1723621
48. *Robeson, L. M.*, Polymer blends: A comprehensive review., Hanser Verlag, Munich, Cincinnati 2007, pp 1–63.

49. *Huggins, M. L.,* Some Properties of Solutions of Long-chain Compounds. J. Phys. Chem. **46**(1) (1942) 151. doi: http://dx.doi.org/10.1021/j150415a018
50. *Krevelen, D. W. V., Nijenhuis, K. T.,* Properties of polymers: Their correlation with chemical structure; their numerical estimation and prediction from additive group contributions. 4th, completely rev. ed., Part II, Ch. 7, Elsevier, Amsterdam, Boston, 2009 pp 189–227.
51. *Small, P. A*., Some factors affecting the solubility of polymers. J. Appl. Chem. **3**(2) (1953) 71. doi: http://dx.doi.org/10.1002/jctb.5010030205
52. *Coleman, M. M., Serman, C., Bhagwagar, D*., A practical guide to polymer miscibility, Polymer **31**(7) (1990) 1187. doi: http://dx.doi.org/10.1016/0032-3861(90)90208-G
53. *Hoy, K. L*., New Values of the solubility parameters from vapour pressure data. J. Paint. Technol,. **42**(541) (1970) 76.
54. *Yun, H., Sato, H., Zhang, J., Noda, I., Ozaki, Y*., Crystallization behavior of poly(l-lactic acid) affected by the addition of a small amount of poly(3-hydroxybutyrate), Polymer **49**(19) 2008 4204. doi: http://dx.doi.org/10.1016/j.polymer.2008.07.031
55. *Gordon, M., Taylor, J. S.*, Ideal copolymers and the second-order transitions of synthetic rubbers. i. non-crystalline copolymers. J. Appl. Chem. **2**(9) (1952) 493. doi: http://dx.doi.org/10.1002/jctb.5010020901
56. *Schneider, H. A*., The Gordon-Taylor equation. Additivity and interaction in compatible polymer blends. Makromol. Chem., **189**(8) (1988) 1941. doi: http://dx.doi.org/10.1002/macp.1988.021890818
57. *Schneider, H. A. Di Marzio, E. A*., The glass temperature of polymer blends: comparison of both the free volume and the entropy predictions with data. Polymer, **33**(16) (1992) 3453. doi: http://dx.doi.org/10.1016/0032-3861(92)91103-9
58. *Simha, R.,Boyer, R. F.*, On a General Relation Involving the Glass Temperature and Coefficients of Expansion of Polymers. J. Chem. Phys. **37**(5) (1962) 1003. doi: http://dx.doi.org/10.1063/1.1733201
59. *Fox, T. G.*, Influence of diluent and of copolymer composition on the glass temperature of a polymer system. Bull. Am. Phys. Soc. **1** (1956) 123.
60. *Jamshidi, K., Hyon, S.-H., Ikada*, *Y.,* Thermal characterization of polylactides. Polymer, **29**(12) (1988) 2229. doi: http://dx.doi.org/10.1016/0032-3861(88)90116-4
61. B*arham, P. J., Keller, A., Otun, E. L., Holmes, P. A. J*., Crystallization and morphology of a bacterial thermoplastic: poly-3-hydroxybutyrate, Mater. Sci. **19**(9) (1984) 2781. doi: http://dx.doi.org/10.1007/BF01026954
62. *Peng, S., An, Y., Chen, C., Fei, B., Zhuang, Y., Dong, L*., Isothermal crystallization of poly(3-hydroxybutyrate-co-3--hydroxyvalerate), Eur. Polym. J. **39**(7) (2003) 1475. doi: http://dx.doi.org/10.1016/S0014-3057(03)00014-4
63. *Sato, H., Murakami, R., Padermshoke, A., Hirose, F., Senda, K., Noda, I., Ozaki, Y*., Infrared Spectroscopy Studies of CH···O Hydrogen Bondings and Thermal Behavior of Biodegradable Poly(hydroxyalkanoate), Macromolecules **37**(19) (2004) 7203. doi: http://dx.doi.org/10.1021/ma049117o
64. *Sato, H., Murakami, R., Zhang, J., Mori, K., Takahashi, I., Terauchi, H., Noda, I., Ozaki, Y*., Infrared Spectroscopy and X-Ray Diffraction Studies of C[BOND]H…O Hydrogen Bonding and Thermal Behavior of Biodegradable Poly(hydroxyalkanoate), Macromol. Symp. **230**(1) (2005) 158. doi: http://dx.doi.org/10.1002/masy.200551155
65. *Garlotta, D*., A Literature Review of Poly(Lactic Acid), J. Polym. Environ. **9**(2) (2001) 63. doi: http://dx.doi.org/10.1023/A:1020200822435
66. *Sun, Y.-J., Baker, W. E*., Compatibilization Using Low Molecular Weight Reactive Additives, in *Baker, W. E., Scott, C. E., Hu, G.-H*., (Eds), Reactive Polymer Blending. Carl Hanser Verlag GmbH & Co. KG, München 2001, pp 254–289. doi: http://dx.doi.org/10.3139/9783446401747
67. *Noolandi, J*., Homopolymer surfactant for immiscible homopolymer blends, Macromol. Theory Simul **3**(1) (1994) 91. doi: http://dx.doi.org/10.1002/mats.1994.040030108
68. *Wan, Y., Yang, J., Yang, J., Bei, J., Wang, S*., Cell adhesion on gaseous plasma modified poly-(l-lactide) surface under shear stress field, Biomaterials **24**(21) (2003) 3757. doi: http://dx.doi.org/10.1016/S0142-9612(03)00251-5
69. *Ji, Y., Li, X.-T., Chen*, *G.-Q.,* Interactions between a poly(3--hydroxybutyrate-co-3-hydroxyvalerate-co-3-hydroxyhexanoate) terpolyester and human keratinocytes. Biomaterials, **29**(28) (2008) 3807. doi: http://dx.doi.org/10.1016/j.biomaterials.2008.06.008
70. *Yasin, M., Tighe*, *B. J.,* Polymers for biodegradable medical devices. Biomaterials **13**(1) (1992) 9. doi: http://dx.doi.org/10.1016/0142-9612(92)90087-5
71. *Lyatskaya, Y., Dilip, G., Gross, N. A., Balazs, A. C*., Designing Compatibilizers To Reduce Interfacial Tension in Polymer Blends, J. Phys. Chem. **100**(5) (1996) 1449. doi: http://dx.doi.org/10.1021/jp952422e
72. *Colomines, G., Ducruet, V., Courgneau, C., Guinault, A., Domenek, S.*, Barrier properties of poly(lactic acid) and its morphological changes induced by aroma compound sorption, Polym. Int. **59**(6) (2010) 818. doi: http://dx.doi.org/10.1002/pi.2793
73. *Wang, S., Ma, P., Wang, R., Wang, S., Zhang, Y., Zhang, Y*., Mechanical, thermal and degradation properties of poly(d,l--lactide)/poly(hydroxybutyrate-co-hydroxyvalerate)/poly(ethylene glycol) blend, Polym. Degrad. Stab. **93**(7) (2008) 1364. doi: http://dx.doi.org/10.1016/j.polymdegradstab.2008.03.026
74. *Semba, T., Kitagawa, K., Ishiaku, U. S., Hamada, H*., The effect of crosslinking on the mechanical properties of polylactic acid/polycaprolactone blends, J. Appl. Polym. Sci. **101**(3) (2006) 1816. doi: http://dx.doi.org/10.1002/app.23589
75. C*ourgneau, C., Domenek, S., Lebossé, R., Guinault, A., Avérous, L. Ducruet, V*., Effect of crystallization on barrier properties of formulated polylactide, Polym. Int. **61**(2) (2012) 180. doi: http://dx.doi.org/10.1002/pi.3167
76. *Kuusipalo, J*., PHB/V in extrusion coating of paper and paperboard. Part 1. Study of functional properties. J. Polym. Environ., **8**(1) (200) 39. doi: http://dx.doi.org/10.1023/A:1010124205584
77. *Guinault, A., Nguyen, A.-S., Miquelard-Garnier, G., Jouannet, D., Grandmontagne, A., Sollogoub, C.*, The effect of thermoforming of PLA-PHBV films on the morphology and gas barrier properties, in Material Forming – Esaform 2012, Pts 1 & 2, M. Merklein and H. Hagenah, Editors. 2012, Trans Tech Publications Ltd: Stafa-Zurich. pp. 1135–1138.
78. *Gerard, T., Budtova, T., Podshivalov, A., Bronnikov, S*., Polylactide/poly(hydroxybutyrate-co-hydroxyvalerate) blends: Morphology and mechanical properties. eXPRESS Polymer Letters,. **8**(8) (2014) 609 doi: http://dx.doi.org/10.3144/expresspolymlett.2014.64
79. *Robertson, G. L*., Food packaging: Principles and practice. Food science and technology. Third Edition, Taylor & Francis/CRC Press Boca Raton (Fl) 2012, pp 98–123.
80. *Menges, G., Haberstroh, E., Michaeli, W., Schmachtenberg, E*., Menges Werkstoffkunde Kunststoffe. 6. Auflage: Hanser Verlag München 2011, pp 391–424.
81. *Lehermeier, H. J., Dorgan, J. R., Way*, *J. D.,* Gas permeation properties of poly(lactic acid), J. Membrane Sci. **190**(2) (2001) 243. doi: http://dx.doi.org/10.1016/s0376-7388(01)00446-x